2016

Economic Analysis of a Data Center Virtual Power Plant Participating in Demand Response

Labi Bajracharya
South Dakota State University, labi.bajracharya@gmail.com

ECONOMIC ANALYSIS OF A DATA CENTER VIRTUAL POWER PLANT PARTICIPATING IN DEMAND RESPONSE

BY

LABI BAJRACHARYA

A thesis submitted in partial fulfillment of the requirements for the

Master of Science

Major in Electrical Engineering

South Dakota State University

2016

ECONOMIC ANALYSIS OF A DATA CENTER VIRTUAL POWER PLANT PARTICIPATING IN DEMAND RESPONSE

This thesis is approved as a creditable and independent investigation by a candidate for the Master of Science in Electrical Engineering degree and is acceptable for meeting the thesis requirements for this degree. Acceptance of this thesis does not imply that the conclusions reached by the candidates are necessarily the conclusions of the major department.

Timothy M. Hansen, Ph.D.
Thesis Advisor Date

Steven Hietpas, Ph.D.
Head, Electrical Engineering and Computer Science Date

Dean, Graduate School Date

ACKNOWLEDGEMENTS

I would first like to express my gratitude to my thesis advisor, Dr. Timothy M. Hansen for the continuous advice and believing in me from the beginning of my thesis research to its completion. Without his continuous support and feedback, I would not have been able to stand in this position in a short span of time. I would like to take this opportunity to thank Dr. Reinaldo Tonkoski for his valuable advice and suggestion regarding my research work, and helping me to go through times of trouble. Moreover, I would like to thank Dr. Qiquan Qiao for his support in pursuing my Master's degree by believing in me and providing funding for my research work from the Department of Electrical Engineering.

I would like to thank all professors and committee members for providing me valuable suggestions and encouragement. Also, I would like to thank Shekhar and Santosh for their valuable insight into my research work, and to all my friends who made this two years pass with joy.

I am very thankful to my father, Gyanman Bajracharya and mother, Laxmi Bajracharya for their ever lasting love and encouragement to achieve what I dreamt of. Lastly, I owe my wife, Milima for this achievement, by supporting me in every possible way.

CONTENTS

ABBREVIATIONS

CHP	Combined Heat and Power
CPP	Coincident Peak Pricing
CVPP	Commercial Virtual Power Plant
DER	Distributed Energy Resources
DG	Distributed Generation
DOD	Depth of Discharge
DR	Demand Response
EMS	Energy Management System
GHI	Global Horizontal Irradiance
GTI	Global Tilted Irradiance
ISO	Independent System Operator
LMP	Locational Marginal Pricing
OPF	Optimal Power Flow
PV	Photovoltaic
SOC	State of Charge
TVPP	Technical Virtual Power Plant
UPS	Uninterruptible Power Supply
VPP	Virtual Power Plant

LIST OF FIGURES

ABSTRACT

ECONOMIC ANALYSIS OF A DATA CENTER VIRTUAL POWER PLANT PARTICIPATING IN DEMAND RESPONSE

LABI BAJRACHARYA

2016

Data centers consume a significant amount of energy from the grid, and the number of data centers are increasing at a high rate. As the amount of demand on the transmission system increases, network congestion reduces the economic efficiency of the grid and begins to risk failure. Data centers have underutilized energy resources, such as backup generators and battery storage, which can be used for demand response (DR) to benefit both the electric power system and the data center. Therefore, data center energy resources, including renewable energy, are aggregated and controlled using an energy management system (EMS) to operate as a virtual power plant (VPP). The data center as a VPP participates in a day-ahead DR program to relieve network congestion and improve market efficiency. Data centers mostly use lead-acid batteries for energy reserve in Uninterruptible Power Supply (UPS) systems that ride through power fluctuations and short term power outages. These batteries are sized according to the power requirement of the data center and the backup power duration required for reliable operation of the data center. Most of the time, these batteries remain on float charge, with seldom charging and discharging cycles. Batteries have a limited float life, where at the end of the float life, the battery is assumed dead, and require replacement. Therefore, the unused energy of the battery can be utilized by allocating a daily energy budget limit without affecting the

overall float life of the battery used in data center for the purpose of DR. This is incorporated as a soft constraint in the EMS model, and the extra use of battery energy over the daily budget limit will account for the wear cost of the battery. A case study is conducted in which the data center is placed on a modified version of the IEEE 30-bus test system to evaluate the potential economic savings by participating in the DR program, coordinated by the Independent System Operator (ISO). We show that the savings of the data center operating as a VPP and participating in the DR program far outweighs the additional expense due to operating its own generators and batteries.

CHAPTER 1 INTRODUCTION

1.1 Background

The rapid increase in global cloud-scale services has resulted in a similar increase in the number of data centers. The servers and support infrastructure necessary to run these data centers consume significant amounts of energy [1]. In 2013, it was estimated that data centers used 91 TWh of energy — the equivalent of 34 large coal-fired power plants running at peak capacity for the year — with projections to 139 TWh in 2020 [2]. At the same time, the United States Energy Information Administration predicts a 24% increase in residential electricity use and a 31% increase in commercial electricity use — part of which comes from data centers — from a 2013 reference case to the year 2040 [3]. This unprecedented growth in energy usage is occurring at a pace that far outstrips the increase in the available transmission capacity of the power grid. As the amount of demand on the transmission system increases, network congestion reduces the economic efficiency of the grid and begins to risk failure. Additionally, studies show that small and targeted reductions in peak demand can have large impacts on wholesale electricity prices [4].

Demand response (DR) can play a significant role in reducing electricity usage during peak periods and reduce the retail price of the electricity. Furthermore, reducing peak demand provides not only economic benefits, but also helps decrease carbon emissions. In areas where the generation, transmission, and distribution capacity is limited, DR can act as a valuable tool to balance supply and demand. There is a potential to reduce 20% of the total peak electricity in the US through DR programs [5]. It is estimated that in 2019, if DR is implemented, the peak load of the system can be reduced

by 150 GW, which is equivalent to the power production of 2,000 peaking power plants (assuming each of 75 MW plant capacity). This can result in economic savings of about 1.5 trillion dollars [5]. DR providers capable of reducing their electric demand (load) can participate in the Independent System Operator (ISO) day-ahead, real-time, and ancillary service markets. Demand side resources offer bids that reflect their flexibility to adjust their load in response to market conditions. In this thesis, locational marginal pricing (LMP) at the bus connected to the data center is used to trigger a DR signal from the ISO. Because data centers are highly automated, monitored, and consist of flexible loads, they can participate in DR programs.

Data centers demand 100 percent availability for all of their applications. Tier level IV data centers, as defined by Uptime Institute [6], can achieve availability up to 99.99%. To minimize the effect of outages, data centers often use redundancies in their energy infrastructure, e.g., backup diesel or natural gas generators, uninterruptible power supplies (UPS) in the form of batteries and flywheels, renewable sources such as photovoltaic (PV) solar. By intelligently managing the data center energy infrastructure, significant energy savings can be achieved. Performing this energy management in data centers will result not just in individual data center energy savings, but will have significant benefits to the grid in reliability and economic efficiency. To that end, a data center energy management system (EMS) is proposed to utilize the data center as a virtual power plant (VPP). Data centers are abundant, high power loads that are spatially distributed and have the required energy infrastructure making them ideal VPP candidates. VPP EMS coordinates the power output of generators, energy storage, and controllable loads [7]. VPPs consist of distributed energy resources that can be used to make contracts and bids in the wholesale

market and offer services to the ISO. The proposed VPP EMS analyzes the economic benefit of participating in DR to reduce network congestion (physical security) and reducing energy costs to the system and the data center.

Data centers mostly use lead-acid batteries for energy reserve in UPS systems that ride through power fluctuations and short term power outages. Vented (flooded) batteries, Valve Regulated Lead Acid (VRLA) batteries, and Modular Battery Cartridge (MBC) are the different types of lead-acid batteries in use today in data centers. These batteries are sized according to the power need of the data center and the backup power times required for reliable operation of the data center. Most of the time, these batteries remain on the float charge with a small number of charge and discharge cycles. It is also known that the batteries have limited life regardless of its use or not, and this life before the battery is being termed dead is called the float life of the battery. Therefore, the unused energy of the battery can be utilized without affecting its overall float life for the purpose of DR. The average outage duration of the grid is considered while calculating the unused energy. In this light, unused capacity of the battery energy storage can be properly utilized with economic benefits in return for the services to grid.

Today, data centers are incorporating renewable sources, such as PV and wind, to reduce carbon footprint and energy prices, but their intermittent nature is a challenge. Data centers will either have their own renewable energy source or buy it from existing off-site generation. Apple has already deployed two large solar farms that produce 40 MW of solar power in Maiden, North Carolina, and is planning to add another 17.5 MW solar panel farm in the nearby city of Claremont, North Carolina. Similarly, Microsoft is buying 110 MW of wind energy from a wind farm to power its San Antonio data center. The

problem with renewable sources in the EMS model are the uncertainty in the forecast of renewable power. In this work, solar power has been considered as a source of renewable energy in the data center. The variability and uncertainty of PV can be a challenge while making unit commitment decisions of the generator, so a stochastic optimization framework for the EMS model of the data center VPP has been developed to take into account the uncertainty of the PV output based on the forecast error distribution. A number of scenarios are generated to capture the uncertainty of the solar forecast, and then subsequently reduced to ease the complexity and reduce the computation time.

1.2 Contributions

The main contributions of this thesis are stated below:

(a) feasibility study of data center VPP participating in DR when network conditions are considered

(b) proposed daily battery energy limit model based on float life, depth of discharge, and power system outage data, and

(c) quantification of economic savings for both the electric power system and data center VPP participating in DR from reducing the system peak and relieving network congestion.

1.3 Thesis outline

This thesis has been organized as follows: Chapter 2 lists the different literatures available in the field of DR in data center, data center VPP, and battery management in data center. Chapter 3 defines the concept of VPP which forms the basis for data center VPP, and the description of its components. Chapter 4 presents VPP component models,

DR savings calculation model, and a VPP optimization model to study a case of data center VPP participating in DR in a modified IEEE-30 bus test system. Chapter 5 introduces an improved battery cost model integrated into a modified VPP optimization model and case studies in the modified IEEE-30 bus test system. Chapter 6 presents a stochastic optimization model which accounts for the uncertainty of PV source in day-ahead scheduling. Lastly, Chapter 7 presents the conclusion, limitations, and future developments related to the research thesis.

CHAPTER 2 LITERATURE REVIEW

This chapter explores literature related to data center DR using different techniques such as shifting of workloads and use of local generation, VPP concepts and energy storage device management inside the data center.

There has been a lot of work in the field of data center DR or demand side management considering scheduling of workload utilizing the spatial-temporal differences of geographically dispersed data centers. DR capability of internet data centers was studied in [8]. They made use of shifting delay tolerant batch jobs among data centers located in three different market areas based on the LMP price and the cooling efficiency of the data center. Similarly, in [9], performed scheduling of batch jobs in geographically distributed data centers, not on the basis of electricity price alone, but also considered the fairness factor among different organizations. They even considered maximum server inlet temperature as a constraint to prevent server heating. Likewise, electricity cost reduction in data center by reducing the number of active servers, and finding optimum service rate of server in geographically distributed data centers has been studied in [10]. In [11], risk aware DR program was developed for geographically located data centers to operate data centers as controllable load resource in the electricity market. Workloads are migrated in the form of virtual machines based on the LMP price of the market, and the main focus is on the data center getting economic reward based on which type of DR the data center is participating, especially real time DR and economic DR. The risk due to uncertainty in the LMP price and network bandwidth fluctuation during transfer is modelled using Markowitz's mean variance method. In all of these study, workload shifting is the main

method of achieving DR among multiple data centers. They have not considered local generation energy resources to assist them in DR.

Opportunities of data center for peak-load shaving as well as integration of large renewable energy into the grid was studied in [12]. The study concluded that data centers can act as a large scale energy storage sites to provide fast-response during times of renewable energy fluctuations. This paper also presents the various challenges data center face that limit its participation in DR programs such as market immaturity and complexity, and risk tolerance of data center being low.

Most DR in data centers prefer to shift power consumption to time and places or from utilities offering lower prices with typical constraint in the form of performance requirement of the incoming workload.In [13], a study was conducted to analyze the impact of using energy stored in batteries to offset the electricity cost of data centers. The author used Lyapunov optimization technique to determine cost optimal solution. Delay tolerant workload management is considered in addition to battery energy model. However, the battery energy model takes into account the capital cost of it, and the battery requirement for the outage has not been clearly taken in the model.

In study [14], the authors used two DR schemes to reduce data center's peak load and electricity expenses. They used coincident peak pricing (CPP) data from Fort Collins Utilities to get warning signals, and developed average and worst case base for predicting uncertainty of the CPP warning. Workload shifting in addition to local backup generator was performed, which resulted in significant cost savings. But, in this paper, battery model was not considered in the problem formulation.

In [15], patented pre-cooling method was utilized to operate data center as a VPP.

The main aim was to reduce grid load during peak time by allowing the data center temperature to rise up up to certain limit to avoid paying higher cost of electricity. Data centers produce considerable amount of heat, a watt of server power requires an additional watt of cooling needs. An EMS can control a data center by either absorbing excess power from the grid during over-generation of power on the grid by storing power within the data center, or reduce power consumption from grid by making use of energy stored in the data center when requested by the ISO. Data center can anticipate these events by using pre-cooling to lower the internal temperature from 80 F to 60 F. The system can then turn off the cooling equipment during the peak load hour, letting the temperature float over to 80 F to avoid paying during high energy cost. The data center will not compromise its service level while doing so. In this work also, local generation resources have not been mobilized for DR purpose.

Bidding strategy of a VPP was formulated in market related to both energy and spinning service in study [16] . This model considers distributed energy resources (DER) such as generators, electrochemical storage placed at different locations in the same geographic location. Genetic algorithm was used to solve the non-linear optimization problem to find the suitable bids considering the DERs operational constraint as well as network constraint. In our work, data center resources are available which can be aggregated to work as a VPP. They are all situated near to the data center peripheries, so network conditions will not have to be accounted. The energy resources can be controlled remotely by the already built-in communication infrastructure present in the data center.

In [17], an EMS for data center was formulated to make the data center work as a VPP. The DERs considered in this study are the backup generators, UPS battery energy

storage. The EMS schedules backup generators and battery for providing day-ahead DR based on a grid set-point. This paper uses fixed electricity retail price to quantify its economic savings due to DR. Also, battery wear cost is applied for energy withdrawal from battery [17]. In this thesis, only the portion of the battery energy which causes battery degradation is applied the wear cost. A daily budget is allocated in which the battery can supply without costing money as well as battery wear. In addition, LMP acts as a signal for DR in the day-ahead market, instead of a fixed retail electricity price.

Various forms of energy storage devices (ESD) such as lead acid, ultracapacitors, flywheel in data centers regarding its suitability, placement and amount of storage, was studied in [18]. This work is related to power provisioning of ESDs based on workload characteristics.

Use of distributed batteries in the data center to reduce both the capital and operational expenditure of the data center was presented in [19]. They used distributed UPS architecture for peak shaving of the data center load, and found out that bigger provisioning of battery backup is beneficial. The UPS batteries stores energy during low activity periods and then use in to reduce power spikes. This help more serves to be provisioned for the same power budget reducing total cost of ownership of server. In a follow-up work in [20], using distributed battery control, they were able to shave 23 MWhr/week of energy in a 10 MW data center at no additional cost.

In [21], dual-purposing of UPS battery energy in data centers for the purpose of power outage and demand response was studied. This work comes with the conclusion that the originally provisioned battery power is sufficient to automatically supply the energy needs for demand response. They also studied about hybrid energy storage

technologies for use in power backup and demand response case, and found it to be more effective than battery alone case. But, this thesis work is concerned with quantifying how much battery energy can be allocated for demand response on a daily basis without degrading the life of the battery.

CHAPTER 3 THEORY

3.1 Virtual Power Plant

Distributed generation (DG) is being used to promote energy efficiency and the use of renewable energy resources, alternative to the conventional generation sources based on coal, nuclear and hydropower plants. The penetration of DER is increasing worldwide associated with more sustainable energy with less environmental problems. The problem with DG is that it is not visible to the grid system operator, although it can replace some proportion of energy needs from the centralized units. Because of its small, isolated modular power source, with an intermittent nature, taking part in energy market is risky. This will result in passive use of DG and can hinder the growth of DG sources. Therefore, the concept of VPP was introduced to aggregate DERs for the purpose of trading electricity or to act as an ancillary service provider. VPP is defined differently under different projects such as Europe Union (EU) virtual fuel cell power plant [22], Fenix project etc.

According to EU project of virtual fuel cell power plant, VPP is defined as a group of interconnected decentralized residential micro-CHPs, using fuel cell technology, installed in multi-family houses, small enterprises, public facilities etc., for individual heating, cooling, and electricity production [22]. Similarly, based on [23], VPP is a flexible representation of a portfolio of DER. A VPP not only aggregates the capacity of many diverse DERs, it also creates a single operating profile from a composite of the parameters characterizing each DER and incorporates spatial constraints on aggregate DER output, as shown in Fig. 3.1. A VPP is composed of different types and numbers of

DERs with various availability.

In this thesis, VPP is a cluster of DG units, controllable loads, and energy storage systems, aggregated to operate as a unique power plant. The generators in this description can be both fossil and/or renewable energy source. A VPP is an EMS which coordinates the power flows coming from DERs. The EMS can work based on the needs such as minimization of generation costs, maximization of the profit, or minimization of the green house emissions. A VPP system is based on software and a smart grid to remotely and automatically dispatch and optimize DER via an aggregation and optimization platform that links retail to the wholesale market [24].

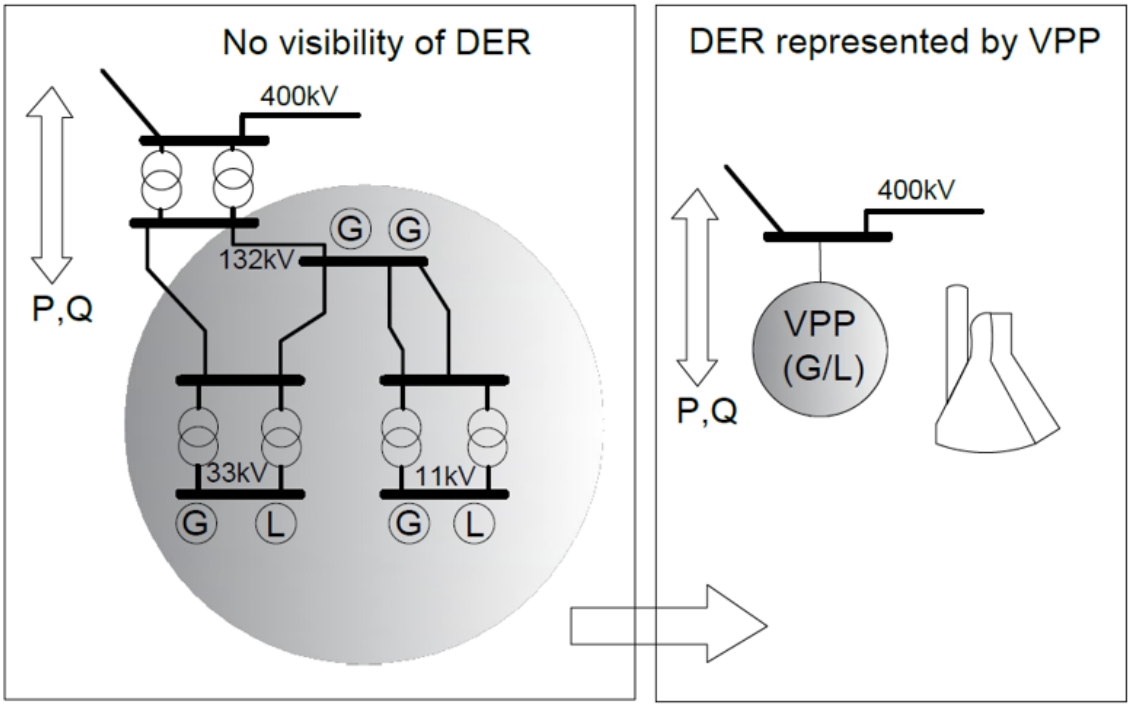

Figure 3.1. VPP concept in FENIX [25]

3.1.1 Classification of VPP

VPP can be used for energy trading in the wholesale markets, and can also provide various types of ancillary services such as frequency and voltage regulation. Therefore, based on the activities such as market participation and system management and support, VPP can be classified into two types, the commercial VPP (CVPP) and technical VPP (TVPP), respectively [23].

3.1.1.1 CVPP

CVPP is a representation of DER that can take part in energy markets similar to conventional generating units. Clustering small DERs into a single entity will reduce risk in market participation while enhancing diversity of energy resource and increased energy capacity. However, the DERs should be geographically close to take part in a LMP-based markets.

3.1.1.2 TVPP

TVPP is an aggregator of DER which works at the transmission boundary level so that it is visible to the system operator. The input to the TVPP is the information on DER in the local network that is passed by various CVPPs. This facilitates distribution system operator to aggregate the operating setpoints, parameters, and cost data from each DER in the network along with detailed network (topology, constraint, etc.) information, and hence calculate the contribution of each DER forming the TVPP. TVPP will facilitate use of DER capacity and provide scheduled ancillary service capabilities.

3.1.2 VPP components

Ideally, the VPP consists of three major parts, which are categorized as follows [26].

3.1.2.1 Generation Technology

There are several DER technologies that can be considered for integration into a VPP. They are listed as below:

- natural gas generators
- diesel generators
- biomass and biogas
- combined heat and power (CHP)
- wind power
- solar power
- controllable load etc.

The DGs may serve individual consumers for residential, commercial or industrial sectors. Owner of the DGs may inject surplus of the production to the grid, and in times of shortage, can be imported from the grid. Some DGs which are owned publicly may have the sole purpose of injecting its production to the grid. Generally, the DGs may be accompanied by energy storage devices. Also, some of the DGs may have stochastic nature, such as wind and solar, which are not equipped by energy storage devices. Fuel cells and micro-turbines are dispatchable as they are capable of changing their operating set-points quickly. Therefore, the DGs may be further classified as Dispatchable DGs and Stochastic DGs.

3.1.2.2 Energy storage technologies

Energy storage plays a crucial role in managing power balance and stability. It is combined with renewable power sources for smoothing out the fluctuations or variations by storing surplus energy during high renewable generation and dispatching it during power shortage scenario. So, it can act as a buffer in case of non-dispatchable or stochastic generation. Some of the technologies that can be considered for integration in VPP are listed below:

- battery energy storage system
- flywheel energy storage system
- supercapacitor energy storage
- hydrogen along with fuel cell
- hydraulic pumped energy storage system

3.1.2.3 Information communication technology

Communication plays a vital role in the modernization of the electric power system. Proper communication scheme is required for two ways transfer of information between field devices and the main control unit. Similarly, Data center VPP requires communication infrastructure to get input from various DERs to its EMS. It further requires information from the ISO for the operating set-points, which the EMS uses to run some sort of optimization to schedule its DER accordingly.

3.1.3 Data Center VPP

Data centers are suitable candidates to operate as a VPP, mainly because data centers have underutilized energy resources such as diesel/natural gas generators, large

battery banks, and renewable energy sourcess like wind and PV solar, which provides the flexibility to participate in the energy market [17]. The number of data centers are increasing, and are spread across the electric power network, so there are variations in the spatial-temporal dimension. In addition, the capacity of today's data centers is large. For example, Facebook's data center in Prineville, Oregon has a capacity of 28 MW, which is nearly the amount of power that is being used by all homes and business in the rest of the Oregon county where the data center is located. According to Greenpeace [27], Apple's data center in North Carolina is estimated to consume 100 MW of power, equivalent to 80,000 U.S. homes.In addition, data center loads are flexible, and in study [28], it was found that 10% of the total load can be curtailed within 15 minutes for demand side management.

Similarly, the data center can take advantage from workload shifting among data centers located at different geographic location as shown in Fig. 3.2. The real-time electricity price, nature of grid power (dirty or green), renewable availability across data centers may influence the transfer of workload.

In this thesis work, DR mechanism is performed considering only backup generators, UPS batteries and renewable energy sources which are the major components of the VPP. Fig. 3.3 shows the block diagram of the VPP. A data center VPP consists of natural gas generators, lead-acid battery and PV as renewable source, and are described individually.

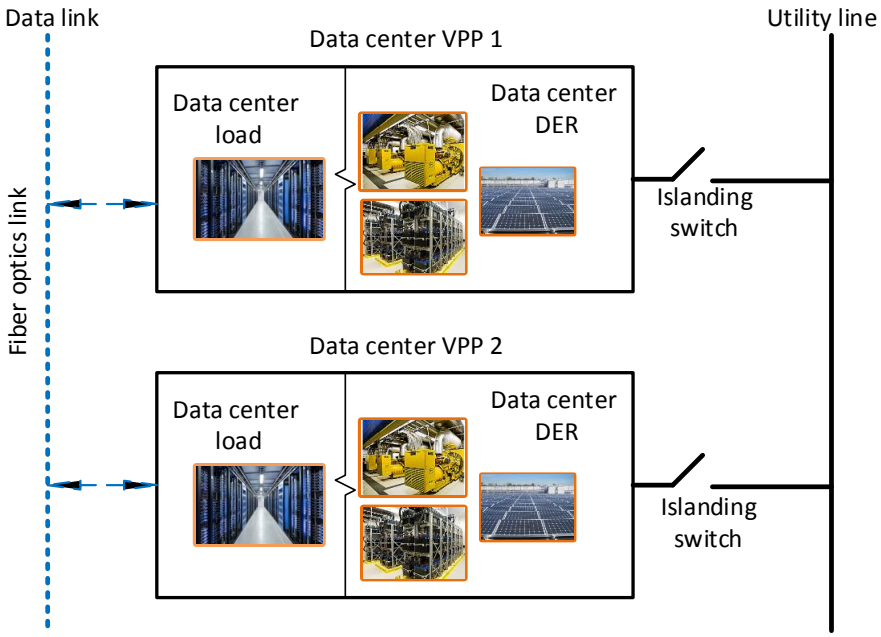

Figure 3.2. Multi VPP framework [17]

3.1.3.1 Photovoltaic (PV) system

PV system is comprised of a large number of PV modules, which in turn is made up of semiconductor device known as solar cell that convert sunlight into direct current electricity. Power produced from PV panel is not linear, as it depends upon the operating voltage. Maximum power occurs at the knee of the I-V curve as shown in Fig. 3.4. If I_m and V_m represents the cell current and cell voltage at maximum power, P_m, then the maximum power is the product of those two quantities. In Fig. 3.4, I_{SC} represents the short circuit current through the solar cell when it is short-circuited, and V_{OC} represents open circuit voltage, which is the maximum output voltage when no load is connected.

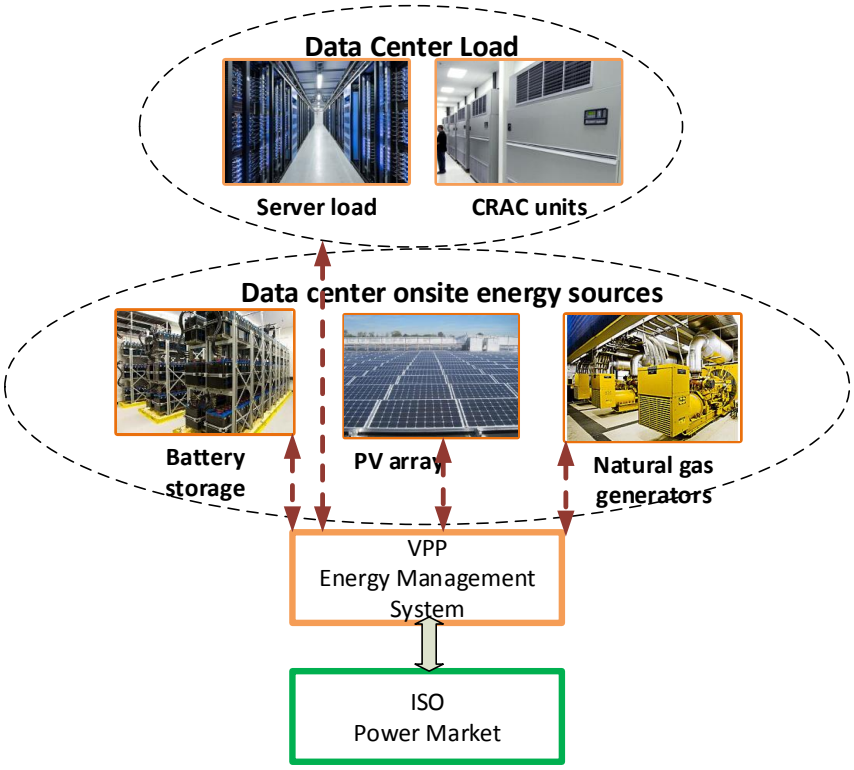

Figure 3.3. Data center VPP consists of server and computer air room conditioning (CRAC) units as data center load; on-site energy sources such as battery storage for UPS, PV array, and backup generators; VPP EMS communicates with the ISO for coordinating its load and energy resources to take part in DR.

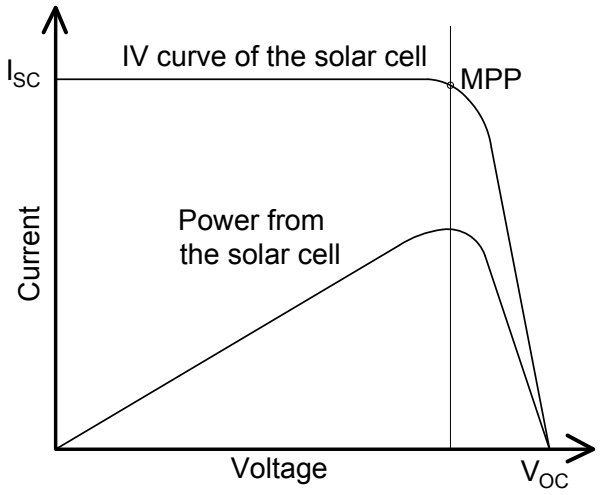

Figure 3.4. I-V characteristic curve of solar cell [29]

The I-V characteristic of PV cells differ under different illumination or solar irradiance levels as shown in Fig. 3.5. The short circuit current depends upon the irradiance and the temperature of cell. Most system employ maximum power point tracker (MPPT) to track the optimum operating point where the power generation is maximum. MPPT has a feedback system to sense the PV power output and, in effect change the array output voltage until the output power is maximum. Neglecting the effect of temperature on the PV module, the PV power output from the PV nominal capacity of P_{nom} is given as in Eq. 3.1. In Eq. 3.1, G_T and $G_{T,STC}$ denote the solar radiation incident on the solar panel and the incident radiation at standard test conditions (STC). The STC for characterization of PV cell is an irradiance of 1000 W/m^2 at air mass (AM) of 1.5 and cell temperature of 25°C.

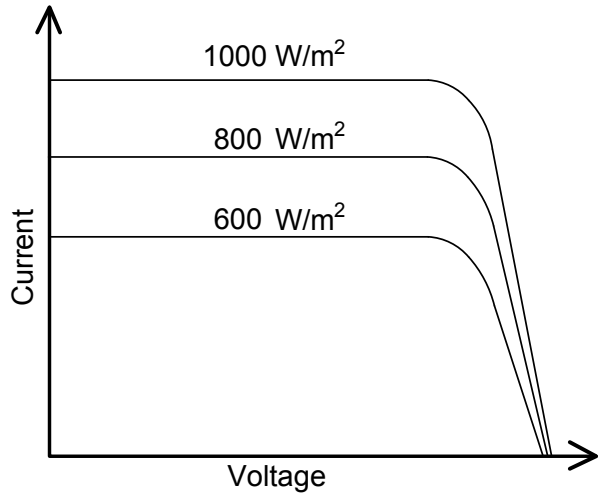

Figure 3.5. I-V curve of a PV module at different irradiance levels

$$P_{PV} = P_{nom}\, f_{PV}\, \frac{G_T}{G_{T,STC}} \tag{3.1}$$

3.1.3.2 Natural gas generator

Data centers contain emergency backup generation that can power the load within 10-15 seconds when a grid outage occurs. Because the frequency of outages is not significant in today's grid, most of the time the generators are idle. Therefore, these underutilized generators, along with storage and renewable energy sources, can be operated as a VPP. The amount of fuel consumption, F by the generator depends upon the generator loading, and is best represented by the quadratic function as shown in Eq. 3.2.

$$F(P_G) = aP_G^2 + bP_G + c \tag{3.2}$$

where $F(P_G)$ is in cu.ft/h; a, b, and c are the fuel curve coefficients of generator whose units are cu.ft./kW^{2}h, cu.ft./kW h and cu.ft./h respectively; and P_G is the power output of the generator in kW.

Natural gas generators, as the name suggests, use natural gas (methane that the utilities supply) to generate electricity. An internal combustion engine gets injected a mixture of fuel and air into a combustion chamber, where a piston compresses the mixture and a spark plug ignites it, which drives the piston down turning the crankshaft. The crankshaft then turns the rotor of the generator in an electromagnetic field, thereby generating electrical power.

Natural gas generator has the most affordable and effective fuel among the non-renewable resources for power generation. The average fuel cost of utility natural gas is around 4.48 dollars per thousand cubic feet, only more expensive than coal as a fuel for power plants. However, coal is one of the highest pollutant and a major source of emission

of green house gases (GHG). Also, natural gas is pumped underground through the extensive network of pipelines in utility scale. Therefore, it can be easier to access during a major disaster such as hurricanes.

3.1.3.3 Energy storage technology

Data centers require energy storage devices to address the risk of interruptions to the main power supply as it is faster to respond than generators. Its application can be divided into three major functional categories as listed below:

- power stability
- power bridging
- energy management

Among the three technologies (batteries, flywheels, and ultracapacitors) that qualify for practical use in data centers, lead-acid batteries are still the mostly widely used because of its advantage in terms of lower capital cost, high energy density,re and longer runtime. Fig. 3.6 shows the capital cost versus the runtime for different energy storage methods.

Data centers have large battery energy storage system which act as a backup device in the form of UPS. They bridge the power outage seamlessly so that power continuity and availability of the data center is maintained. After some predefined time, backup generators come in action if power cut is suspected to be of longer duration. Batteries can be short-term to medium-term sources of stored energy, capable of supporting critical IT load for minutes to hours. Runtime or the energy capacity of the battery can be increased by adding more battery strings in parallel. Batteries are often installed in cabinets next to a UPS, or can be setup in racks or shelves in a dedicated battery room. Of the different

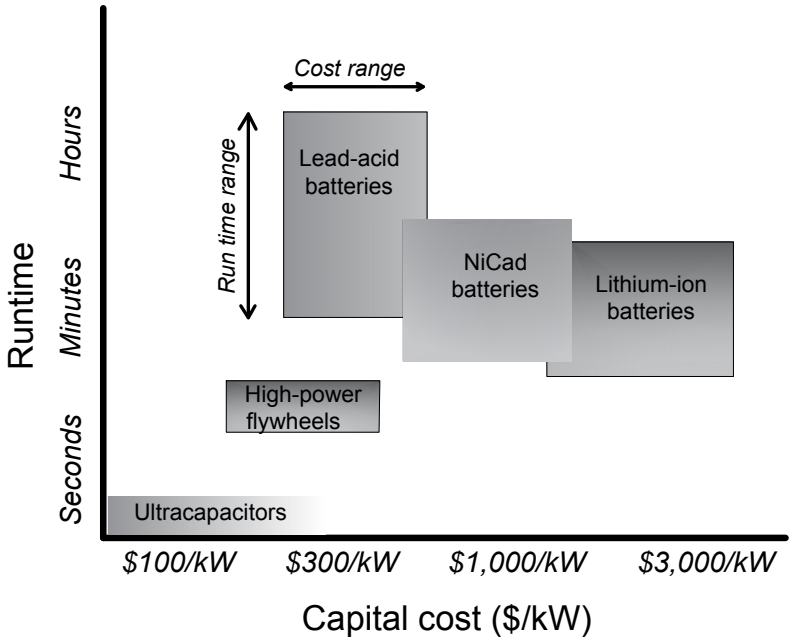

Figure 3.6. Capital cost vs. runtime for energy storage methods [30]

batteries such as lead-acid (both flooded and VRLA), nickel cadmium, lithium-ion, and nickel-metal hydride batteries (Ni-MH), lead-acid batteries are the most common batteries.

The dynamics of batteries are determined by the state of charge (SOC). SOC provides the amount of electrical charge present in the battery based on its initial capacity. The SOC of the battery after time interval $\triangle t$ can be determined by knowing the initial SOC at time period t; battery charge (+ve) or discharge power (-ve); P_{bat} in kW; battery capacity Bat_{cap} in kWh; the duration of discharge $\triangle t$ in hour; and the charge (η_{ch}) or discharge (η_{disch}) efficiency, as shown in Eq. 3.3 and Eq. 3.4.

$$SOC(t+\triangle t) = SOC(t) + \frac{P_{bat}(t) \times \eta_{ch}}{Bat_{cap}} \ , \ where \ P_{bat} > 0 \tag{3.3}$$

$$SOC(t+\triangle t) = SOC(t) + \frac{P_{bat}(t) \times \eta_{disch}}{Bat_{cap}} \ , \ where \ P_{bat} < 0 \tag{3.4}$$

Operating the battery in lower SOC for a longer period of time risks battery life degradation. Not only that, during emergency period, if the SOC of the battery happens to be low, then the reliability of the data center might be compromised. Therefore, the SOC is maintained between the minimum permissible limit SOC_{min} and maximum limit SOC_{max}, as given by Eq. 3.5. At the end of day (i.e., t = T), SOC of the battery is also maintained above some predefined level for its operation in the next day as given by Eq. 3.6.

$$SOC_{min} \leq SOC(t) \leq SOC_{max} \tag{3.5}$$

$$SOC(t > T) = SOC_{nextday} \tag{3.6}$$

3.2 Demand Response

DR is one of the segment of VPP market in which consumption of power is changed to assist the grid. DR is crucial as it enhances market economic efficiency, curtails peak demand, increases grid reliability, and defers transmission expansion. Data center DR is particularly an interesting area as it has the resources that can be utilized for the benefit to both the grid and itself. Data centers represents large loads, but they are also flexible as the load can be shifted in time, location, and even curtailed, although it results in quality reduction. In addition, data centers have full backup resources which are underutilized. Financial benefits as a result from DR participation can help ease the high cost of electricity usage.

Below are some of the promising opportunities for data center to participate in the

DR programs [12].

(a) Time-of-use pricing:

The utility sets the price according to the amount of electricity usage as peak, mid-peak and off-peak hours, each having its own electricity rate.

(b) Peak pricing:

Mostly for industrial and commercial loads, utilities charge an additional price based on the maximum demand.

(c) Coincident peak pricing:

This is based on the peak hour for the utility, where most electricity is requested by the utility from the wholesale supplier. This is opposed to the peak of an individual customer, and the rate for this situation is about 200 times higher than the base case [14].

(d) Day-ahead pricing:

Day-ahead prices are calculated based on the market clearing prices in the wholesale electricity market. Wholesale market provides hourly market prices day-ahead before the actual market operation takes place.

(e) Real-time pricing:

In this pricing mechanism, customers are charged the changing electricity price based on the market clearing every 15 minutes interval.

In this thesis, day-ahead dynamic pricing is considered, where the LMPs in the grid are used to induce DR signal to the data center operator from the ISO.

3.3 Optimal Power Flow

Standard AC optimal power flow (OPF) is used to find the optimization vector consisting of bus voltage angles, magnitudes, and the generator real and reactive power injections. The objective function of OPF is to minimize generation cost while meeting network constraints. The equality constraints constitute real and reactive power balance equations, and the inequality constraints consist of branch flow limits. Other constraints include bus voltage magnitude bounds and generator magnitude bounds.

LMP for the bus locations can be computed through AC OPF using MATPOWER [31]. LMPs can vary due to congestion in the line and hence use of more expensive generators. Thus, it incurs more cost to deliver the same amount of power to the load. Relieving congestion in the transmission network can be accomplished by reducing the bus load through DR mechanism, which is the main task of this thesis. In this thesis, a 28 MW data center is placed on a power system along with a time-varying lumped load to study the economics when data center performs DR to induce system-wide savings along with reduced energy costs for the data center.

CHAPTER 4 ECONOMIC ANALYSIS OF DATA CENTER VPP

This chapter describes the data center benchmark model to study data center as a VPP. The data center VPP energy resource cost model is explained in detail. In addition, the data center VPP EMS optimization model is designed to schedule generators day-ahead based on grid-setpoint.

4.1 Data Center benchmark model

A benchmark model is required to study the various cases. In this thesis, the data center benchmark is built-up from the study [17]. The data center considered is a Tier IV topology as defined by Uptime Institute [6]. Tier IV topology provides complete redundant system with two active power delivery paths. Also, there are N+1 UPS and generator for backup purpose.

The data center is assumed to be located in Colorado for the test case. The power capacity of the data center was assumed to be 28 MW, based on the test case which will later be described in Section 4.5. This amount of power is reasonable for a data center, as real data centers have power in this range. Also, 10 MW PV solar is assumed to be installed, and supplies a certain portion of green energy to the data center.

The data center has 28 MW of backup natural gas generator installed to handle the peak power of the data center. The data center will house 22.08 MWh of flooded lead-acid battery energy storage for 1-hour backup duration. The capacity of the battery storage unit was calculated based on the peak IT power requirement. The data center load breakdown, such as IT load, cooling load, etc., was based on the report provided by Lawrence Berkeley National Laboratory (LBNL), as shown in Fig. 4.1.

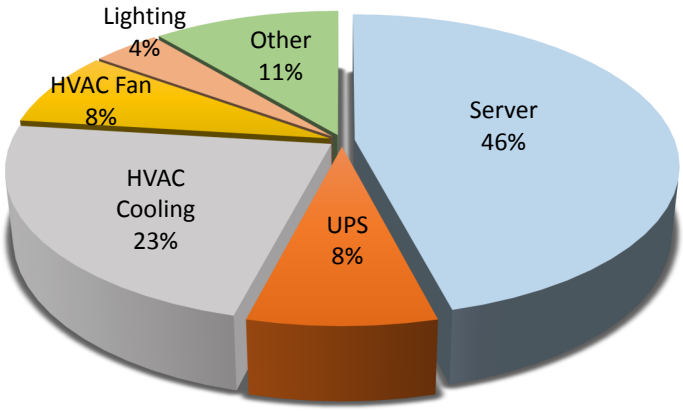

Figure 4.1. Average breakdown of data center load [32]

4.2 General VPP component model

The energy resources utilized in data center VPP are modeled below.

4.2.1 Solar power model

The input data for the calculation of solar output power is the global horizontal irradiance (GHI), in kW/m^2, which is available from NREL [33]. GHI is then resolved into its beam and diffuse radiation based on the clearness index [34]. GHI is then converted to global tilted irradiance (GTI), which is the solar irradiance incident on the panel surface [35].

A solar PV array having a rated capacity of 10 MW is connected to the data center, located in Colorado for simulation purposes (latitude: 39.77° and longitude: -105.22°). Solar arrays are fixed in position and are assumed to be facing South at a slope equal to the latitude where it is installed. This maximizes the year round performance for a fixed array position. A PV derating factor of 0.8 is assumed to account for the losses due to soiling, shading, snow cover, aging, etc. Using Eq. 3.1, the PV output power can be

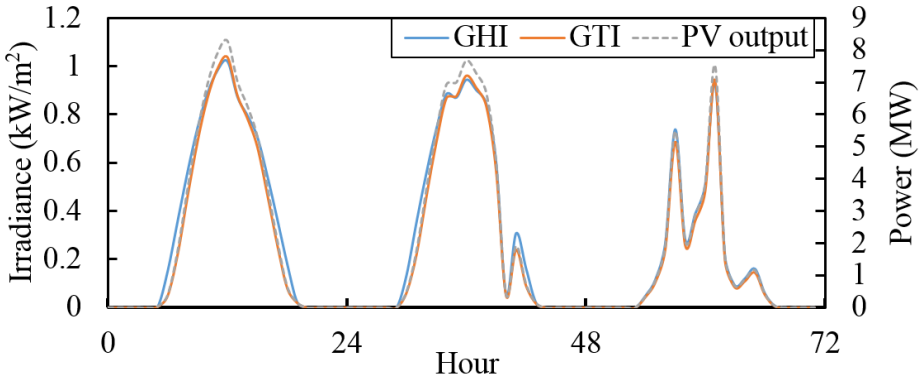

Figure 4.2. Global horizontal irradiance, global incident radiation, and PV output from 07/22/2006 to 07/24/2006

calculated given the GHI.

4.2.2 Natural gas generator cost model

Generator costs include the startup cost, fuel cost and maintenance cost. The generator hourly replacement cost is not considered, because the capital investment cost will not come into play for DR purposes. Likewise, emission cost of generator has been omitted as the natural gas fuel produces less green house gas as compared to diesel engine counterparts. Daily generator fuel cost is represented by the quadratic cost function as given in Eq. 4.1

$$C_i(P_{G,i}) = C_{natural\ gas} \times \sum_{t=1}^{24} (a_i \times P_{G,i}^2(t) + b_i \times P_{G,i}(t) + c_i \times U_{i,t}) \tag{4.1}$$

where i is the generator unit number; C_i is the operating cost of unit in \$/h; $C_{natural\ gas}$ is the price of natural gas in \$/cu.ft.; P_{Gi} is the power output of unit i in kW; a_i, b_i and c_i are the fuel cost coefficients of unit i whose units are cu.ft./kW^{2}h, cu.ft./kWh and cu.ft./h respectively; and U_i is the generator startup binary indicator $\{0,1\}$.

In addition to the fuel cost, generator incurs maintenance costs associated with both

the engine and the generator set, but the majority of maintenance is performed on the engine. Generator units that are not adequately maintained are more likely to break down during critical hours of operation or may not start when called upon. There are different generator service level maintenance such as inspecting and testing engine, gauges and meters, change of engine oil, replacement of fuel and oil filters, maintenance of spark plugs, and many more. These are scheduled from daily inspection to monthly, half yearly and yearly depending upon the level of maintenance. According to study conducted by EPRI [36], they evaluated the annual cost of maintenance over a 20-year period, and found out that the maintenance cost for all level equals nearly 20% of the installed cost of the unit for 20 years. Assuming the cost of a 4.2 MW generator to be $2,295,000, the 20 year net present value cost turns out to be $459,000. Assuming, the generator runs from about 300 to 2000 hours per year, the hourly maintenance cost of the generator ranges from $76 to $11 per hour. In this work, the generator maintenance cost has been taken as $45 per hour of operation. Also, the start-up cost of the generator is taken as a fixed $25 to account for the cost associated with pre-heating the generator, and the time taken to run at full capacity.

Seven 4,000 kW natural gas generators from Caterpillar (CG260-16) are used to power the 28 MW data center. The average fuel cost of natural gas is 4.475 dollars per thousand cubic feet. Table 4.1 shows the fuel consumption of the natural gas generator as specified in manufacturer's data-sheet, and the fuel cost ($/h) for corresponding to the generator loading [37].

Table 4.1. Natural Gas Generator Fuel Cost Data

Power (kW)	Efficiency (%)	Fuel Consumption (cu.ft./h)	Fuel Cost ($/hr)
4,000	43.8	31,682.1	141.2
3,000	42.5	24,502.8	109.2
2,000	40.2	17,271.3	77.0

Each generator's maximum and minimum output is set to 4,000 kW and 1,000 kW, respectively, to operate in the high efficiency region. Fig. 4.3 shows the fuel curve of a single 4 MW natural gas generator cost of the natural gas generator is linearized by the data available from Table 4.1 and is given as

$$C_i(P_{Gi}) = 0.0321P_{Gi} + 12.788 \tag{4.2}$$

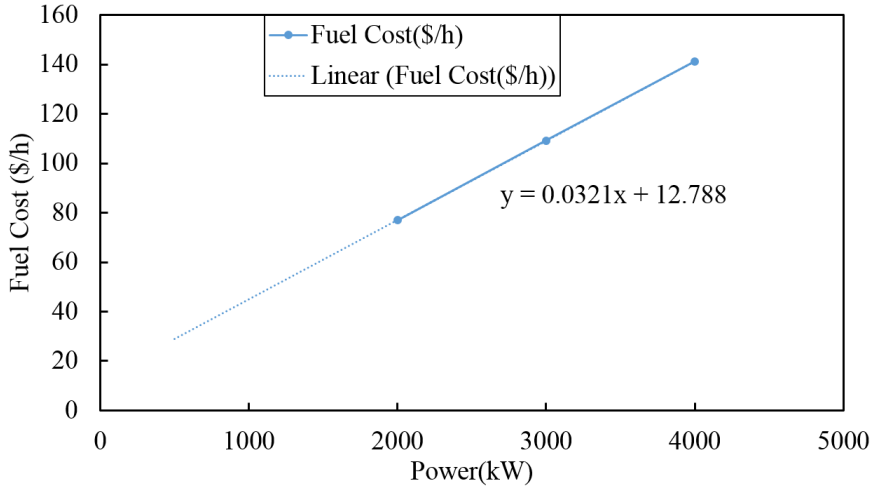

Figure 4.3. Fuel curve of a 4 MW natural gas generator

4.2.3 Data Center load

In general, a data center load depends on server workload and cooling needs. The incoming workloads and outer temperature changes throughout time causing fluctuation in data center power. The reference for the data center load was based on the NREL data center load in [38]. Since the variation in the data center load is relatively small, a constant load of 28 MW was assumed to match the IEEE 30-bus test system used in this thesis.

4.3 DR model

The data center participates in a day-ahead DR program by obtaining a DR signal from ISO. Let T be the time scale of the study, which is 24 hours; N_{bus} be the total number of load buses; L_j^b and L_j^a are the LMPs of the load bus j before and after DR in \$/MWh, respectively; P_j^b and P_j^a are the power of the load bus j before and after DR in MW, respectively; P_{dc}^b and P_{dc}^a are the net data center load (total data center load - renewable generation) before and after DR in MW, respectively. The total power system savings, computed as in Eq. 4.3, from to the reduction in LMPs for all the load buses because of DR by data center VPP EMS is given as S_{sys}. Similarly, S_{dc} denotes the energy savings to the data center through the reduction in LMP via DR, determined as in Eq. 4.4.

$$S_{sys} = \sum_{t}^{T}[\sum_{j}^{N_{bus}}(L_j^b \cdot P_j^b) - \sum_{j}^{N_{bus}}(L_j^a \cdot P_j^a)] \tag{4.3}$$

$$S_{dc} = \sum_{t=1}^{T}[(L_j^b \cdot P_{dc}^b) - (L_j^a \cdot P_{dc}^a)] \tag{4.4}$$

4.4 VPP optimization model

VPP EMS day-ahead optimization model schedules the operation of backup generators to minimize generation cost. Optimization was implemented in IBM ILOG CPLEX optimization studio, and the objective model and constraint are given as in Eq. 4.5 and Eq. 4.6 respectively.

$$\min_{P_{Gi},U_i} \sum_{t=1}^{T} \sum_{i=1}^{N_g} C_i(P_{Gi}) \tag{4.5}$$

where, N_g is the total number of generators; U_i is the binary variable indicating ON/OFF of generator i.

$$\sum_{i=1}^{N_g} P_{Gi,t} + P_{PV,t} + P^a_{dc,t} - P_{sc,t} = 0 \tag{4.6}$$

$$U_i \cdot P_{Gi,min} \leq P_{Gi} \leq U_i \cdot P_{Gi,max} \tag{4.7}$$

where, at time t, $P_{Gi,t}$ is the generation of unit i, $P_{PV,t}$ is the output from solar panel, $P_{sc,t}$ is the total data center load; $P^a_{dc,t}$ is the net data center load after DR; $P_{Gi,min}$ and $P_{Gi,max}$ are the minimum and maximum power that can be delivered by generator respectively. All the units of power are in kW.

If the solar output differs from what was forecasted during real-time operation, the data center generators will have been rescheduled so that appropriate power is provided, or else pay a penalty, if DR cannot be provided.

4.5 Test case

A data center operating as a VPP is studied in the modified IEEE 30-bus test system. A scenario is generated in the grid where the data center has to perform DR as a VPP to gain benefits to the grid and to the data center itself by relieving congestion. The data

center EMS gets a day-ahead DR signal from the ISO as a grid-set-point for each hour of the day, and accordingly optimizes the generator scheduling based on available renewable generation from Eq. 4.5. Powering data center from the natural gas generators reduces the amount of load the data center consumes, hence relieving congestion from the grid at the peak time and, ultimately, reducing LMPs across the buses in the network through DR.Fig. 4.4 shows the output power of the 10 MW solar array estimated using Eq. 3.1 for solar GHI data from July 22, 2006 [33]; the net load of the data center is the difference between total data center load and solar output. The data center also has seven, 4 MW natural gas generators as shown in Fig. 3.3.

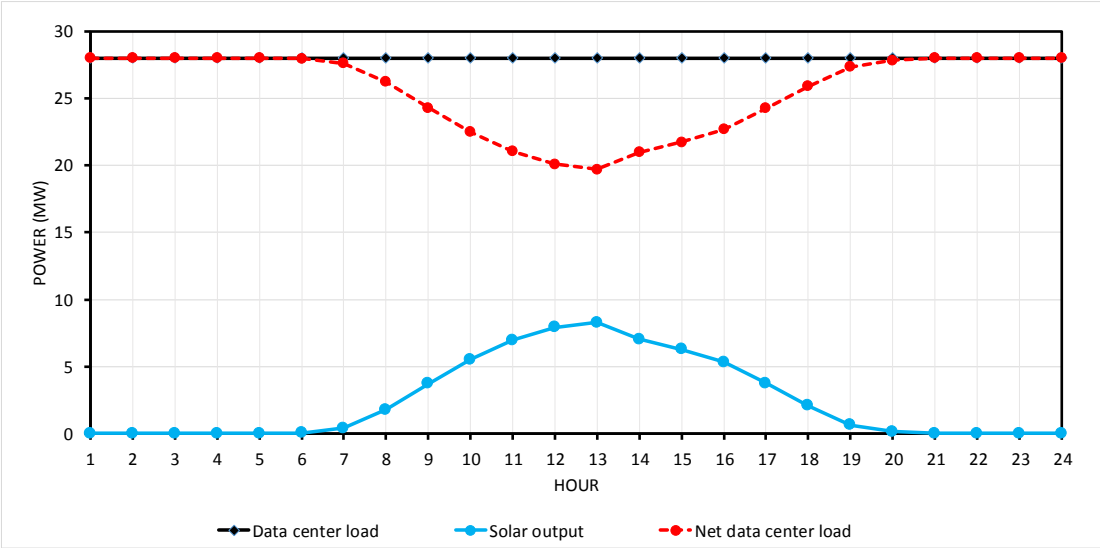

Figure 4.4. Net load of data center, computed as the difference between total data center load and the solar generation.

4.5.1 Modification of IEEE 30-bus test case

Modified IEEE 30-bus system is taken from MATPOWER [31],[39],[40] as shown in Fig. 4.5. It has six generators along with default quadratic cost function coefficients, generator limits, and transmission line constraints.

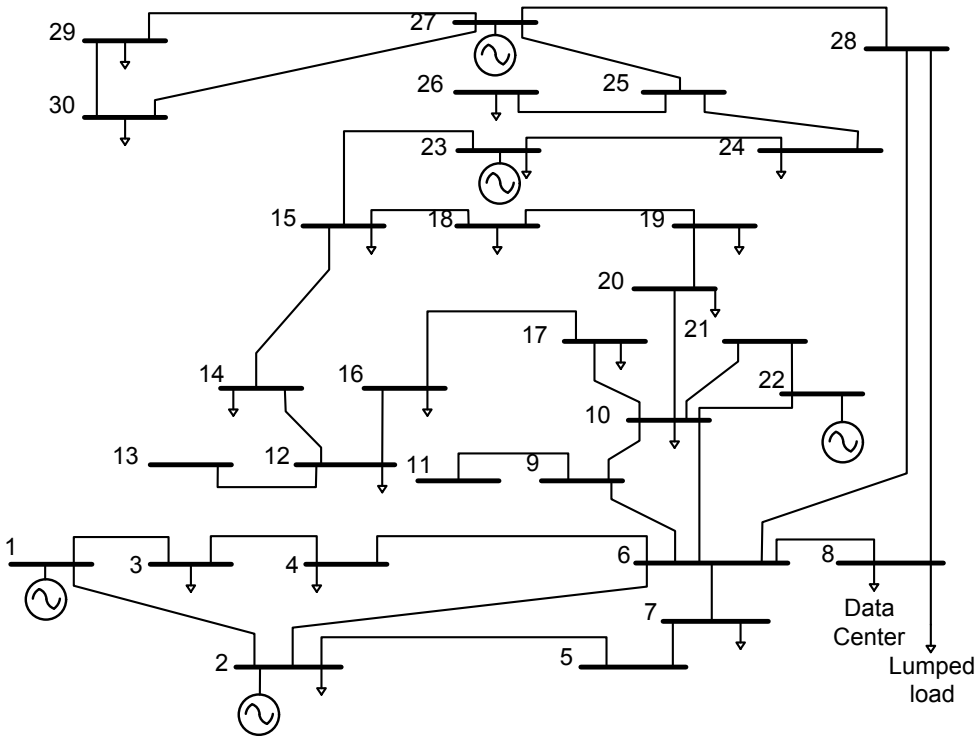

Figure 4.5. IEEE 30 bus system with data center and lumped load at Bus 8 [39].

Using the default cost coefficient, the LMP of the system was determined to be 3.789 $/MWh. The average power plant operating expense for fossil fuel, averaged from year 2003 to 2012, was calculated to be approximately 31.995 $/MWh [41]. To match the average generator operating cost of 31.995 $/MWh, the coefficients of the original cost functions from the IEEE 3-bus test system were scaled so the resulting non-congested LMP was 30.314 $/MWh.

Load at bus 30 was increased from 10.6 MW to 20 MW to introduce more congestion in the transmission system. It was found that Bus 8 was the most sensitive to variations in LMP as a function of load. When the load on Bus 8 reaches 32 MW, the OPF fails to converge, indicating a network failure. In addition to reduced energy costs, in this

case, the DR prevents system failure. Based on these results, data center having a maximum power of 28 MW was considered on Bus 8. The data center was located near the sensitive bus in this case study as part of the feasibility analysis. A scaled commercial load having peak power of 8.7 MW with the hourly profile, shown in Fig. 4.6, was taken from the database of HOMER Pro Microgrid Analysis Tool 3.3.3 software [42]. This lumped load is connected to Bus 8 to create the congestion scenario between the lumped load and the data center.

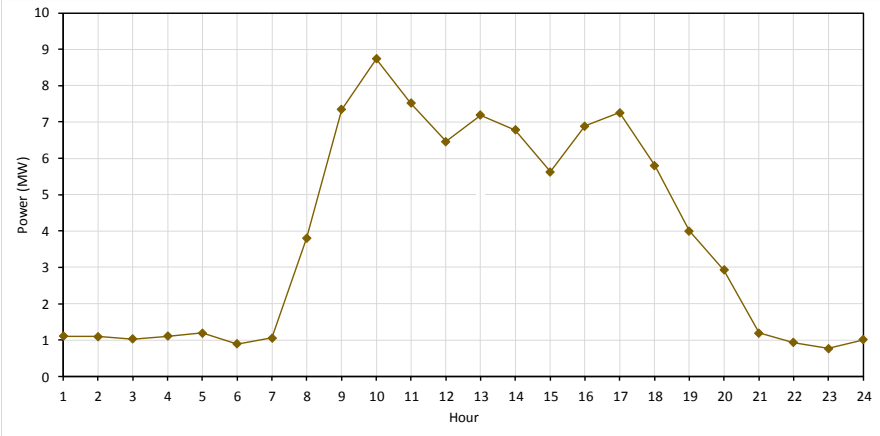

Figure 4.6. Lumped Commercial load at Bus 8 for a day.

As shown in Fig. 4.7, the LMP variation in Buses 8, 25, 26, 27, 28, 29 and 30 due to the 2 MW increment in load at Bus 8 is very high. If the data center can provide DR during this situation, the total system cost can be reduced by relieving the congestion in overloaded transmission lines. Data center can work as a VPP by utilizing its own back-up generators without threatening its own reliability to help relieve grid congestion, and avoid high LMPs at all buses (including the LMP at the data center).

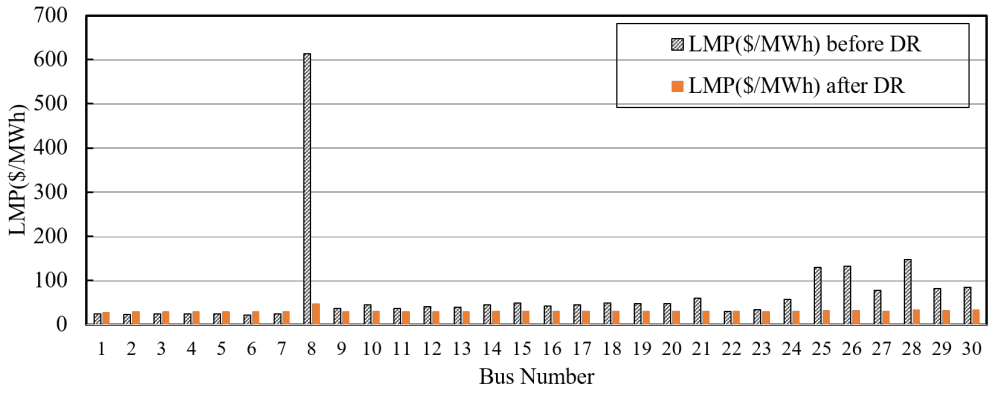

Figure 4.7. Comparision of LMP at all buses before and after DR for a case where Bus 8 load decreases from 32 MW to 30 MW.

4.6 Results

The case presented in the previous subsection shows the load on Bus 8 results in an inefficient market, as shown in Fig. 4.7.The ISO wants to bring the load down to 30 MW by using the data center VPP for DR and sends an appropriate DR signal. Fig. 4.8 shows a case before DR where the lumped load and net data-center load are in the market inefficient zone, which results in a system cost of $190,219. To relieve the congestion in the system, the ISO sends the DR signal to the data center to reduce their load as seen from the grid. After performing DR, the system cost is $156,678, resulting in a total system saving of S_{sys} =$33,541, calculated from Eq. 4.3. VPP reduced the load of the data center by using the natural gas generators optimally by solving Eq. 4.5, and is shown by the shaded area in Fig. 4.9. The total generator operation cost for the day-ahead DR response is $353, so the total energy savings as seen by the data center is S_{dc} =$23,375, calculated from Eq. 4.4. Additionally, the ISO may provide additional incentive to the data center for its participation in the DR program, but that is left for future consideration. If the solar output differs during real-time, then the savings to the data center may change.

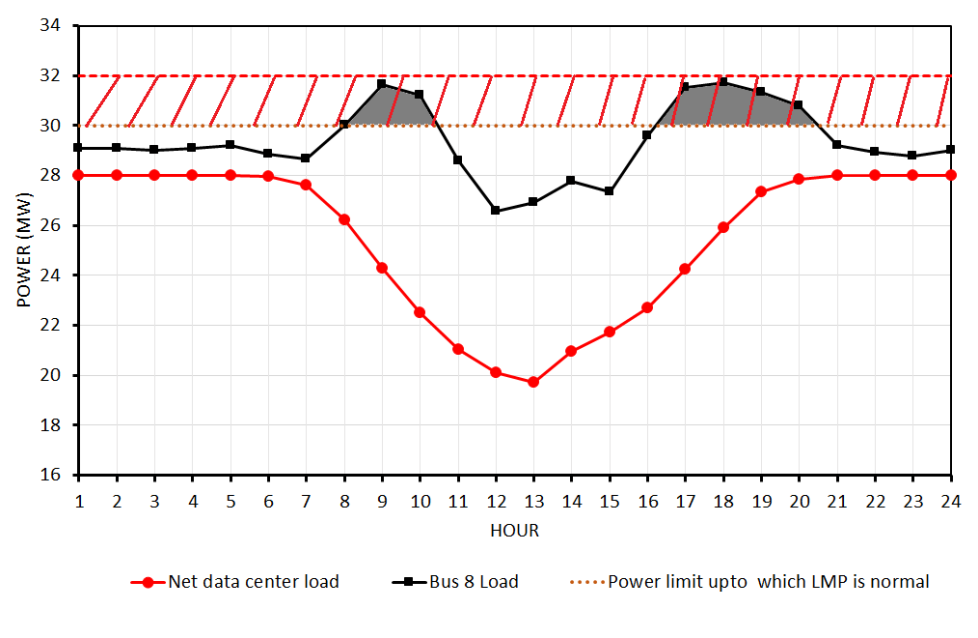

Figure 4.8. The hashed region shows the market inefficient region before DR; grey area represents the load at Bus 8 where congestion and hence market inefficiency occurs, for the entire day.

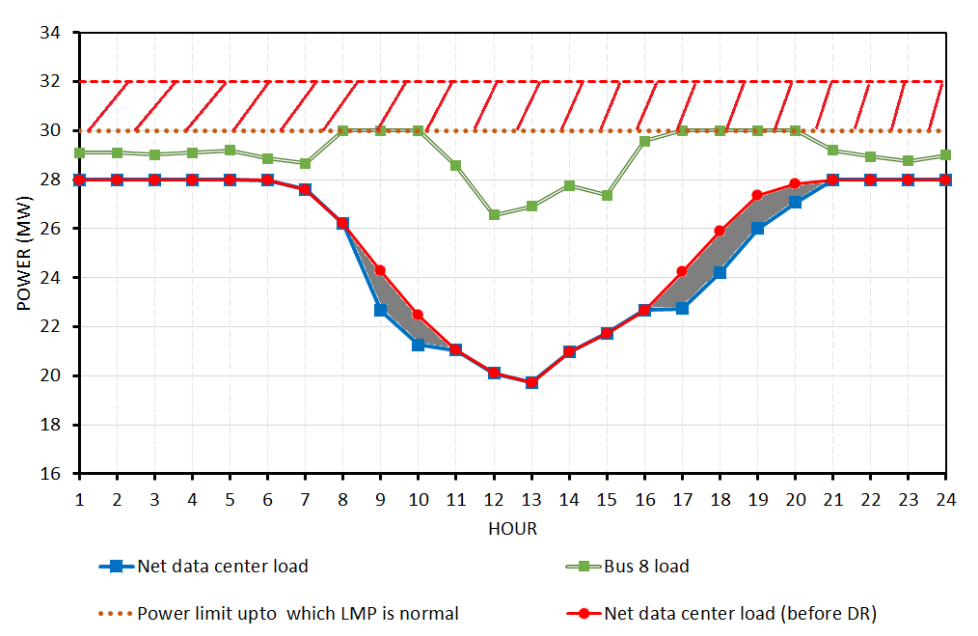

Figure 4.9. The shaded area shows the generator output of the data center to reduce the load on Bus 8 to 30 MW for the DR case.

CHAPTER 5 IMPROVED BATTERY COST MODEL

5.1 Overview of battery energy storage

Conventionally, data center's energy storage devices in particular lead-acid batteries have been utilized for temporary power outage. UPS battery generally supply the power instantaneously upon grid failure, and continue its supply until the backup generator comes into operation. The generator start time delay is generally setup in the 3 to 5 seconds range, and the actual time required for full generator power can be 10 to 15 seconds. The battery capacity is sized such that even in the worst case scenario where all of the generators fail to startup during emergency period, the battery can handle the outage for duration ranging from 5 minutes to a hour based on the provision of energy capacity according to data center requirement. Therefore, the energy stored in the battery can be leveraged for DR purpose, in addition to its primary purpose mainly for power backup.

Battery degradation occurs throughout its useful life based on the frequency of its charge and discharge cycles, depth of discharge (DOD), incomplete or rare charging, high ambient temperature, and various aging processes. As the frequency of power outages are few times a year, the batteries do not quite come to operation. The ampere-hour capacity of the battery degrades over time, and when it reaches to 80% of its initial capacity [43], the battery is termed dead. Furthermore, batteries have their own float life, which is the life time of battery in years, at the end of which the battery should be replaced. So, it can be seen that the battery energy will be unused to a greater extent, and probably wasted by the end of its float life. Therefore, the battery energy can be utilized for DR purpose such that its life-cycle is not significantly affected.

Therefore, in this thesis, to utilize the unused battery energy, daily battery budget has been allocated for DR purposes. The allocated battery energy will not cause battery degradation as it takes into account the float life of the battery. In addition, the allocated energy will also not affect the performance during power outage case, which is the main purpose of having battery storage in the first place. In the following Section 5.1.1, a model has been developed to find the daily allocated battery throughput for the purpose of DR. In Section 5.1.2, battery wear cost has been formulated, and in Section 5.2, VPP optimization model has been formulated using daily battery energy discharge as a soft-constraint with a penalty cost associated with using more battery energy above the daily battery energy limit in the objective function, along with associated dynamics of the battery as constraints.

5.1.1 Calculation of lifetime throughput of battery

The lifetime throughput of the battery is the total amount of energy a battery can produce during its lifetime. It is the fixed amount of energy that can be cycled before the battery requires replacement. Lifetime throughput can be expressed in Ampere-Hour (AH) or in kilowatt-hour (kWh), which can be calculated by knowing the life-cycle, DOD and the battery capacity, all of which can be determined from the battery manufacturer's specification sheet. Fig. 5.1 shows the life-cycle corresponding to various DOD (%) for a lead-acid battery from C&D technology.

The lifetime AH of a battery unit can be computed using Eq. 5.1 [44].

$$AH_{lifetime}(or\ TP) = L_{cycle,DOD_R} \times DOD_R \times C_{bat,AH} \tag{5.1}$$

where, DOD_R is the rated DOD of the battery (in percent), L_{cycle,DOD_R} is the life-cycle at a

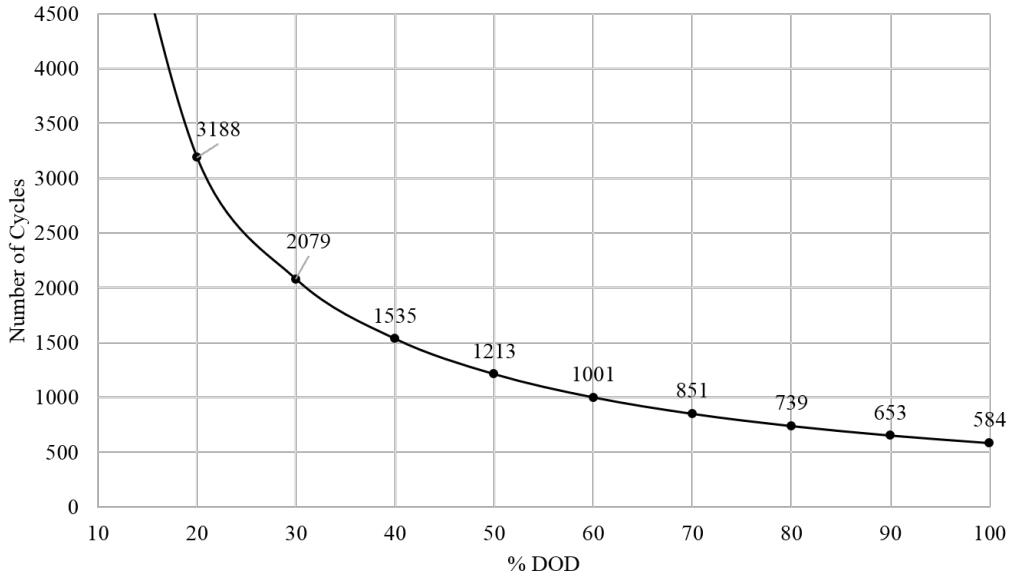

Figure 5.1. Life cycle vs DOD of a lead-acid battery (based on discharges at 1-hour rate to minimum voltage of 1.67 Vpc)

given DOD, and $C_{bat,AH}$ is the battery capacity in AH. A battery will not operate at a single DOD its entire life, so it is hard to determine the $AH_{lifetime}$. In this work, the average lifetime throughput (TP) of the battery is considered which depends upon the average DOD and the average capacity of the battery as given by Eq. 5.2.

$$TP_{avg} = L_{cycle,DOD_{avg}} \times DOD_{avg} \times C_{bat,avg} \tag{5.2}$$

The average lifetime throughput is allocated both to DR and the power outage scenario. The average DOD is based upon the DOD during DR and also during power outage. Power outage is more demanding in terms of power, as the battery backup system has to handle the entire IT load until backup generator starts. In this case, worst case scenario is realized and the battery backup is expected to discharge to its full DOD. But there are only occasional power outages. On the other hand, DR needs to handle only partial load, but

may need to run for hours based on day-ahead DR signal. So, the DOD during DR may not be considerably lowered given the high capacity sizing of the battery bank. The average DOD can be calculated as shown in Eq. 5.3. It can be solved iteratively using Gauss-Seidel method.

$$DOD_{avg}^{(i)} = DOD_{DR}^{(i)} \times \frac{TP_{DR}^{(i)}}{TP^{(i)}} + DOD_{Outage} \times \frac{TP_{Outage}}{TP^{(i)}} \tag{5.3}$$

where,

$$TP_{avg}^{(i)} = L_{cycle,DOD_{avg}}^{(i)} \times DOD_{avg}^{(i)} \times C_{bat,avg} \tag{5.4}$$

$$TP_{Outage} = Yearly\ Outage(hours) \times Current \times Float\ life(years) \tag{5.5}$$

$$TP_{DR}^{(i)} = TP^{(i)} - TP_{Outage} \tag{5.6}$$

$$TP_{DR,daily}^{(i)} = \frac{TP_{DR}^{(i)}}{float\ life\ in\ days} \tag{5.7}$$

$$DOD_{DR}^{(i)} = \frac{TP_{DR,daily}^{(i)}}{C_{bat,avg}} \tag{5.8}$$

In Eq. 5.4, $L_{cycle,DOD_{avg}}$ can be found by knowing the equation of the cycles vs. DOD curve as shown in Fig. 5.1. Likewise, $C_{bat,avg}$ is the average of the initial rated battery capacity and the final battery capacity, which is 80% of the initial rated capacity. This is performed so as to not overestimate the amount of battery that can be used throughout its lifetime. Priority is given to the power outage case where a certain amount of the battery's lifetime energy is allocated to it. The battery energy allocation for power outage is based upon the average duration of grid outage per year, and is given by system average interruption duration index (SAIDI). SAIDI represents the total duration of an

interruption for the average customer during a given time period. The value of SAIDI is 244 minutes per year according to a study by [45]. The float life of the battery based on manufacturer's specification is 20 years. Using higher value of float life will assure that a much greater portion of the battery energy will be allocated to the outage case as shown by Eq. 5.5. Not only that, it will result in a minimum energy allocation for the DR, which will reflect in terms of having low DOD. Eq. 5.6 represents the throughput energy of the battery to be used for DR purpose, whereas the daily throughput energy of battery is calculated from Eq. 5.7. Similarly, Eq. 5.8 finds the average depth of discharge due to DR.

5.1.2 Battery wear cost calculation

Since data centers have already made huge investment in backup power systems, the capital cost should not be accounted for every amount of energy drawn by the battery. In Section 5.1.1, daily energy was allocated to the battery for the purpose of DR. Withdrawing the allocated amount of energy will not lead to significant battery degradation as it takes into account the depth of discharge of the battery. But, using battery energy above the allocated limit will lead to degradation of the battery, if it happens on a regular basis. Therefore, some additional cost must be accompanied to the use of extra energy from the battery, which is denoted by $C_{batWear}$ in this thesis. The battery wear cost will determine the overall operational cost of data center as a result of its usage. This will be considered in the EMS optimization model as it will affect the dispatch of generator and battery accordingly to minimize overall operational cost. Eq. 5.9 gives the battery's average lifetime throughput in terms of average kWh throughput.

$$TP_{kWh} = \frac{TP_{Ah} \times Battery\ Voltage_{nom}}{1000} \tag{5.9}$$

Therefore, battery wear cost in $/kWh can be calculated as given in Eq. 5.10.

$$C_{batWear} = \frac{Capital\ Investment(\$)}{TP_{kWh} \times \eta_{disch}} \tag{5.10}$$

5.2 Modified VPP optimization model

The modified VPP EMS day-ahead optimization model schedules the operation of backup generators along with battery set-points to minimize overall operational cost of DR. The objective function for this problem is given as:

$$\begin{aligned} \min_{P_{Gi},U_i,P_{Bat}} (\sum_{t=1}^{T} (\sum_{i=1}^{N_g} C_i(P_{Gi}) + MC \times U_{i,t} + SUP \times Y_{i,t}) \\ + LMP_{grid,t} \times P_{dcNetLoad,t}) + C_{batWear} \times P_{batExtra} \end{aligned} \tag{5.11}$$

Following are the contraints for the optimization model:

i) Power operational range

$$P_{sc,t} - \sum_{i=1}^{N_g} P_{Gi,t} - P_{PV,t} + P_{bat,t} \leq P_{dcmax,t}\ \forall t \in T \tag{5.12}$$

$$P_{sc,t} - \sum_{i=1}^{N_g} P_{Gi,t} - P_{PV,t} + P_{bat,t} \geq P_{dcmin,t}\ \forall t \in T \tag{5.13}$$

ii) Generator loading limits

$$U_i \cdot P_{Gi,min} \leq P_{Gi,t} \leq U_i \cdot P_{Gi,max}\ \forall t \in T, \forall i \in N_g \tag{5.14}$$

iii) State of charge limit of battery

$$SOC_{min} \leq SOC_{bat,t} \leq SOC_{max}\ \forall t \in T \tag{5.15}$$

iv) State of charge at the end of day

$$SOC_{t=T} \geq SOC_{end\ Day} \tag{5.16}$$

v) Battery energy allocation soft constraint

$$\sum_{t=1}^{T} P_{batDischarge} - P_{batExtra} \leq P_{dailyBudget} \tag{5.17}$$

$$-P_{batExtra} \leq 0 \tag{5.18}$$

vi) Battery charging and discharging rate limit

$$P_{bat,maxCharge} \leq P_{bat,t} \leq P_{bat,maxDischarge} \; \forall t \in T \tag{5.19}$$

where,

t	Time of day in hour
N_g	Number of generators
MC	Hourly maintenance cost of generator ($)
SUP	Startup cost of the generator ($)
$U_{i,t}$	Generator unit i ON/OFF binary variable
$Y_{i,t}$	Generator unit i startup binary variable
$P_{sc,t}$	Data center load at t (kW)
$P_{Gi,t}$	Power generation by generator unit i at t (kW)
$P_{Gi,min}$	Mimimum power generation limit of generator unit i (kW)
$P_{Gi,max}$	Maximum power generation limit of generator unit i (kW)
$P_{PV,t}$	PV power production at t (kW)
$P_{bat,t}$	Battery power production at t (kW) (-ve for discharging and +ve for charging)

$P_{dcmax,t}$	Maximum operation range of data center at t (kW)
$P_{dcmin,t}$	Minimum operation range of data center at t (kW)
$LMP_{grid,t}$	LMP at bus connected to data center at t (\$/kWh)
$P_{dcNetLoad}$	Net load consumed by data center from grid at t (kW)
$C_{batWear}$	Battery wear cost(\$/kWh)
$SOC_{bat,t}$	state of charge of battery at t
SOC_{min}	minimum allowable state of charge of battery
SOC_{max}	maximum allowable state of charge of battery
SOC_{endDay}	state of charge of battery at the end of the day
$P_{batDischarge}$	Battery discharge power (kW)
$P_{batExtra}$	Extra amount of battery energy above the daily budget (kWh)
$P_{dailyBudget}$	Daily budget allocated to the battery (kWh)
$P_{bat,maxCharge}$	Maximum charge rate of the battery (kW)
$P_{bat,maxDischarge}$	Maximum discharge rate of the battery (kW)

The objective function given by Eq. 5.11 minimizes the operational cost of data center while participating in DR as it considers the fuel cost of generator (C_i), the startup (SUP) and maintenance (MC) cost of generator, battery wear cost if operated above the battery energy budget limit ($P_{dailyBudget}$), and the grid cost to supply the net load of the data center which depends upon the LMP of the grid (LMP_{grid}) at that hour. Considering the LMP of the grid allows the data center to use its cheapest alternative to supply its load such as backup generators while also satisfying other constraints.

Eq. 5.12 shows the two power limit constraint for the data center to operate. The

lower power (P_{dcmin}) constraint is provided by the ISO so that power generators of the grid that are running at its base load will not be affected as a result of reducing more power by the data center using its own backup generator. The upper limit (P_{dcmax}) is placed so that the LMP of system will not be increased if data center load combined with the lumped load connected at the same bus increases. Generator loading limits ($P_{Gi,min}$ and $P_{Gi,max}$) are required to ensure that the generators operate at their higher efficiency region while providing power. There are also startup and shutdown constraint of the generator which will prohibit it from shutting down and starting up at that same time instant.

SOC constraint helps to operate the battery always in some predefined charge level so as to guarantee long-life as well as being available to serve load in times of power failure. For the case of lead acid battery the lower bound of SOC (SOC_{min}) is 50%, and the upper bound (SOC_{max}) has been set to 90%. The initial SOC of battery is assumed to be full i.e. 90%. Therefore, there is a constraint as given by Eq. 5.16 that will allow in any case the battery SOC to reach up to 90% by the end of the scheduling window. This allows the battery to be fully charged and be ready for operation in the following day.

Eq. 5.17 represents a soft-constraint, which need not be satisfied but there is a penalty cost associated with the amount of violation. Here, $P_{batExtra}$ is the violation variable, and the penalty cost is the amount of battery wear cost which is introduced in the objective function. Therefore, the amount of battery discharge during the whole day can be less than or equal to the daily budget allocated to the data center.

The battery must be able to discharge to support full IT load during power failure. So, the discharge rate of the battery is set to 1 C hour rate, where C is the capacity of the battery in Ah according to the specification of the battery. The charging rate of flooded

lead acid battery is lower than the discharging rate. In this case, the charging rate is set to C/8 hour rate. The battery discharging rate must not exceed the specified maximum discharging rate, and similarly the battery charging rate must not exceed specified maximum charging rate, which is given by Eq. 5.19.

5.3 Simulation studies of battery cost model

In Chapter 4, only backup generators of data center are considered in the VPP optimization model. In this chapter, simulation studies are conducted taking into account the battery energy and its associated battery dynamics, such as SOC, and battery's maximum charging and discharging rate as given in the optimization model in Section 5.2. In addition, daily battery energy budget has been allocated so that a certain amount of battery energy may be utilized for DR purpose without causing additional cost or degrading the battery, and also maintaining DOD of the battery within certain limits.

5.3.1 Overview

For the simulation studies, the modified IEEE-30 bus test system as described in Section 4.5.1 is considered. In this test system, the data center is connected at Bus 8 along with a lumped load at that same bus, contributing to the total bus power. During the total optimization window schedule, only the data center load and lumped load are time-varying, but the loads at other buses are assumed to be fixed for simulation purposes.

The data center requires day-ahead information about the price of the node or bus in which it is connected. The LMP of 24-hours can be determined by solving OPF using MATPOWER software. The information regarding each hour LMP depends on the bus power connected to data center, and it is not possible to perform OPF using MATPOWER

every time the load level changes while solving the VPP optimization model. Therefore, an approximate LMP curve at Bus 8 has been developed by solving OPF independently of the VPP optimization model, which is as shown by curve *P*1 in Fig. 5.2. Similarly, Fig. 5.2 shows the different piecewise linear price curves, denoted by *P*2 and *P*3 at that same bus, which are fabricated from the original piecewise linear LMP curve, *P*1 to study different cases if the price curve changes. Piecewise linear functions are used to allow solvers using linear programming, such as CPLEX. The price curve *P*1 has a steep slope after bus power reaches 25 MW, and again the slope is steepest after the bus load goes beyond 30 MW. Curve *P*2 has gradual slope until 30 MW, and then increases sharply after that. Likewise, curve *P*3 has gradual slope up to 25 MW, then increases slightly up to 30 MW power, and lastly the slope increases steeper but not steep as that of curve *P*1 and *P*2 at that region.

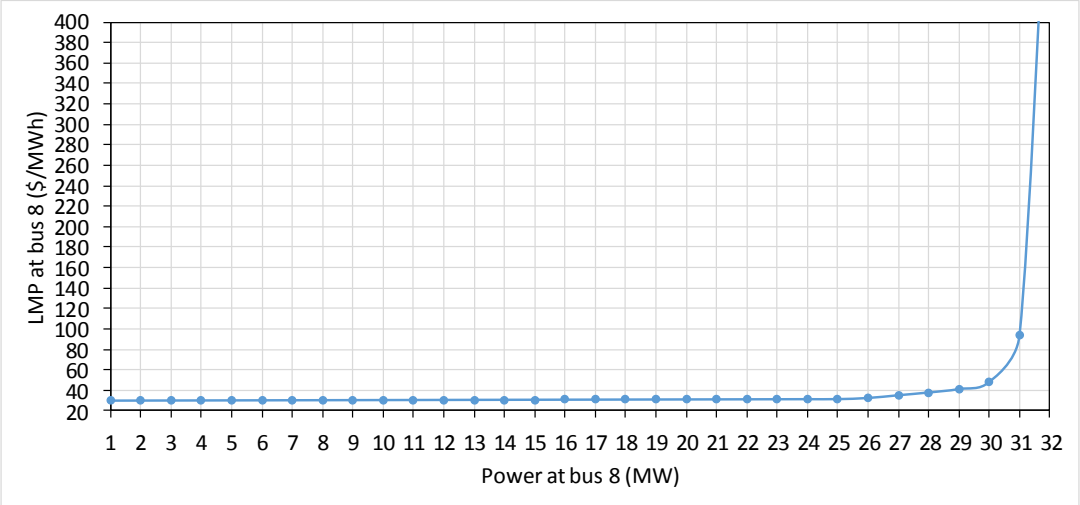

Figure 5.2. LMP curve at Bus 8 showing variation of LMP based on bus power

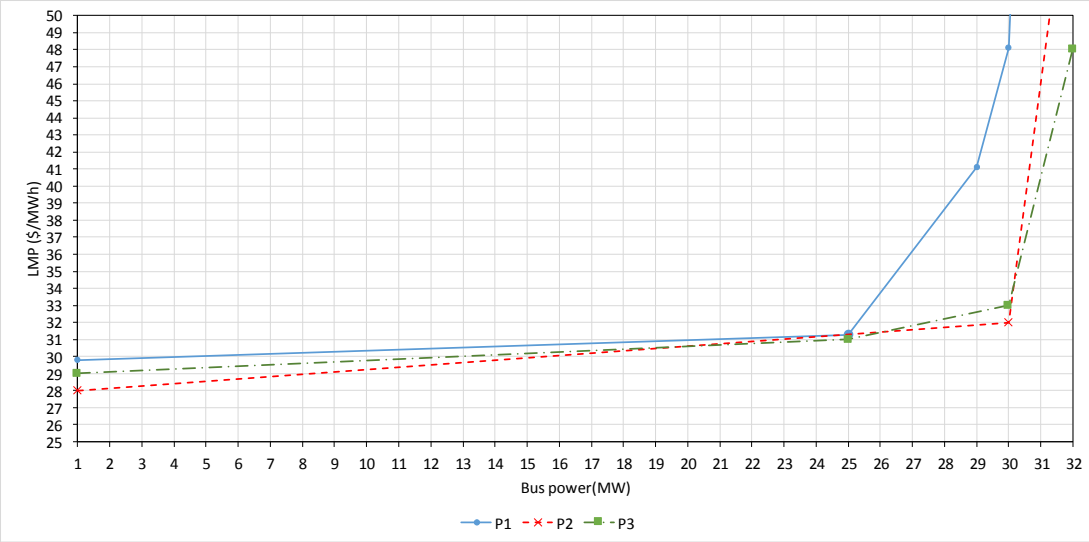

Figure 5.3. Different LMP curves at Bus 8 showing variation based on bus power

The cost of running the backup generator is 32.1 $/MWh with no-load cost of $12.788 as given by Eq. 4.2. Likewise, the startup cost for the generator is assumed to be $25, and the hourly maintenance cost approximated to be $45 as mentioned in Section 4.2.2 . Using the iterative formulation developed in Section 5.1.1, the daily battery energy budget is calculated to be 1780 kWh for the total battery energy capacity of 22,080 kWh. The initial SOC of the battery considered as 0.9, and the SOC at the end of the day is also considered the same. Both the charging (η_{ch}) and discharging (η_{disch}) efficiency of the battery are considered to be 90%. The maximum battery discharging power ($P_{bat,maxDischarge}$) is set to 10 kW and the maximum charging power ($P_{bat,maxCharge}$) as 2 kW. Assuming the total battery investment to be $5,650,000 , the battery wear cost ($C_{batWear}$) is computed to be 0.397 $/kWh using Eq. 5.10.

5.3.2 Case A : 28 MW data center power

The data center load, PV power, and lumped load power are the same as described in Section 4.5. Fig. 5.4 shows the operating ranges provided by the ISO for the data center to operate denoted by $P_{dc,max}$ and $P_{dc,min}$; net data center load before DR; solar power of data center; lumped load connected at the same bus; and total bus power. It shows that the market is inefficient during hours 9 and 10 in the morning, and hours 17 through 20 in the evening. The ISO curtail the peak load, and make the market more efficient by removing congestion in the grid during these times.

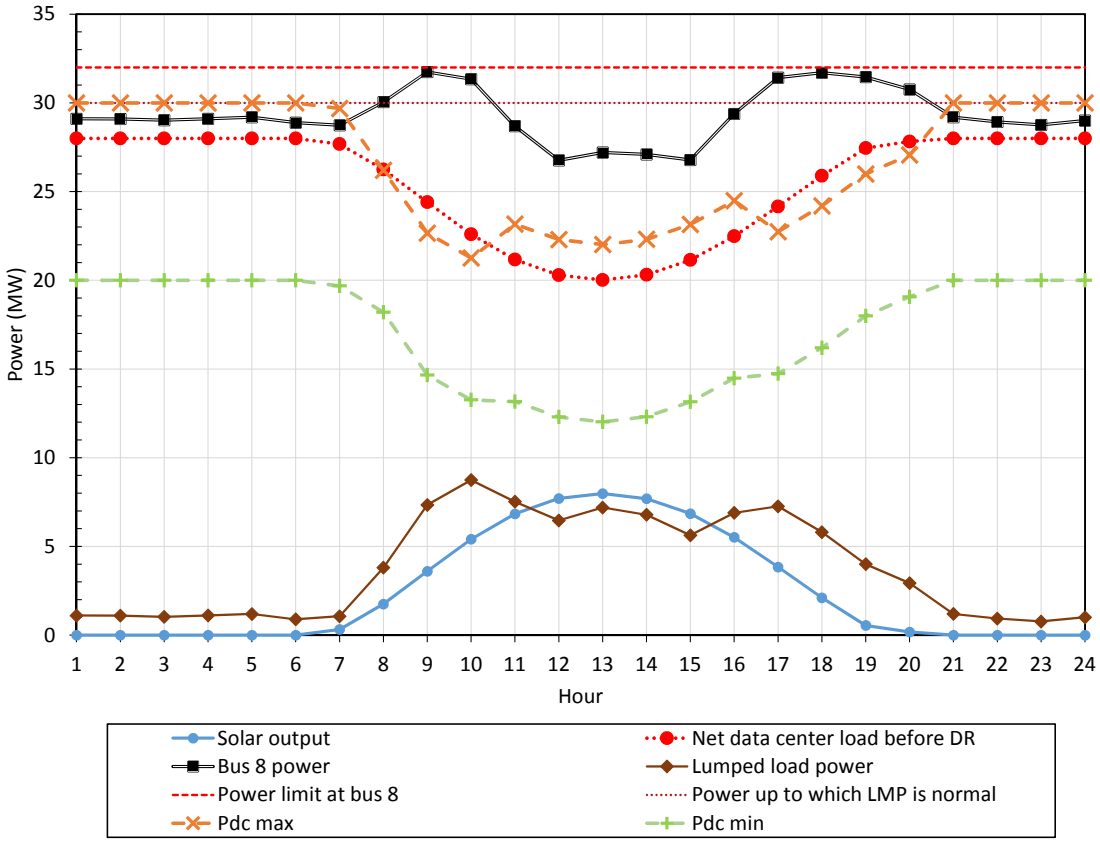

Figure 5.4. Case A input scenario

Three cases based on the different price curves are presented in the following

sections.

5.3.2.1 Case A1: Using price curve P1

The case presented in Section 5.3.2 is solved using IBM ILOG CPLEX Optimization studio by using the objective functions, and constraints developed in Section 5.2, and Fig. 5.5 shows the optimization results overlapped with the input case. As

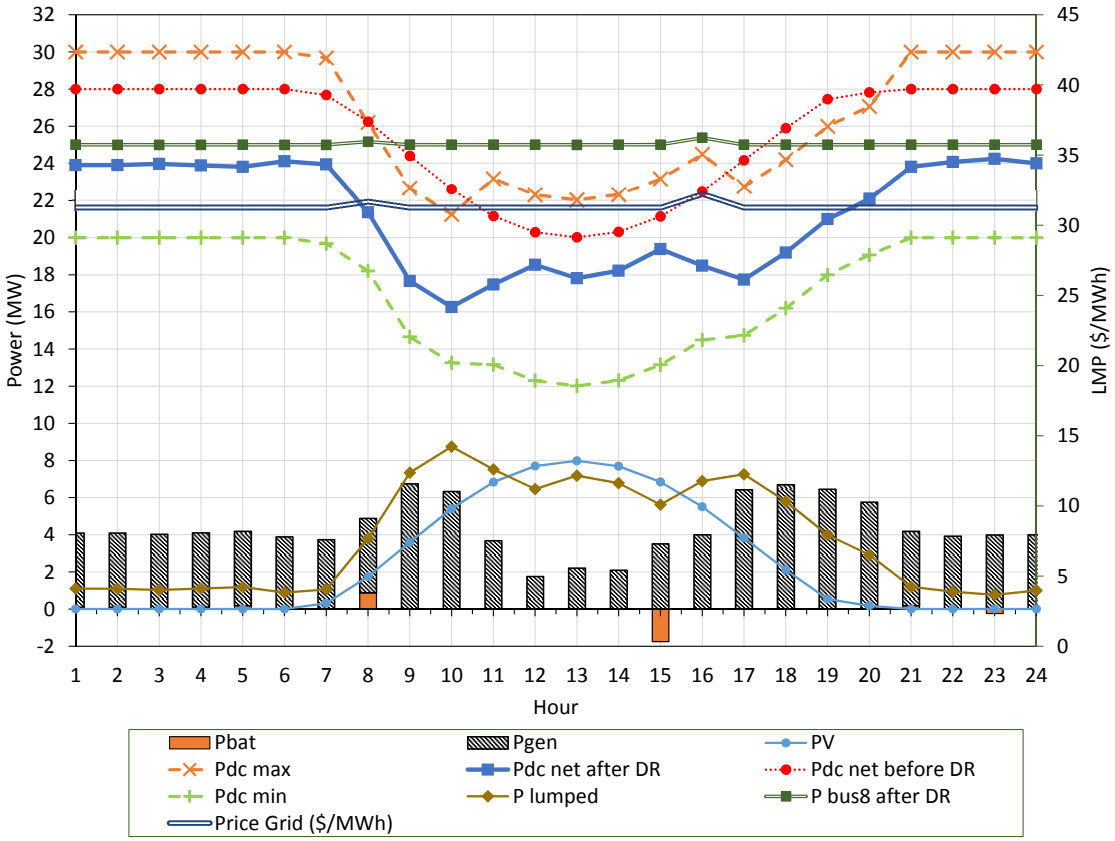

Figure 5.5. Case A1 overall scheduling result

shown in Fig. 5.5, the generators and battery are scheduled in accordance to the data center VPP optimization model. The net load of the data center and the total bus load settles to some value as given by $P_{dcNetAfterDR}$ and $P_{bus8AfterDR}$, respectively. The LMP value of Bus 8 settles to around 31.29 $/MWh as the total bus power is in the range of 25

MW. The net load cannot be further decreased because the cost of operation of backup generators will be higher.

Fig. 5.6 shows the detailed information of the generator and battery scheduling. Positive value of battery power in the diagram means that battery is supplying power or in other words, getting discharged. In this case, during hours 1, 2, 4 ,5, 8, and 21 the battery is being discharged, and during hour 15 and 23 the battery is being charged. The throughput of the battery is 1780 kWh, i.e., all the allocated battery budget has been used for this case. The variation in SOC of the battery can be seen from Fig. 5.7. The lowest SOC reached is only about 0.83 with the depth of discharge of 8.2%.

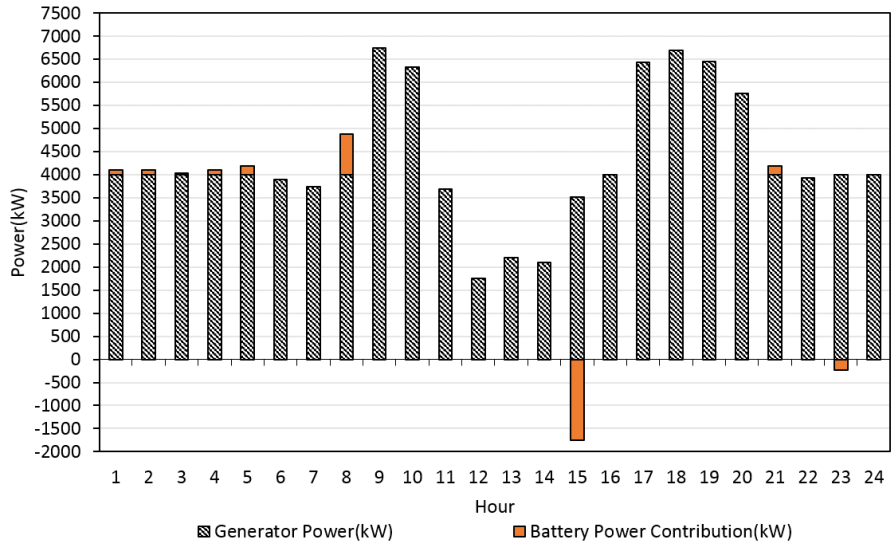

Figure 5.6. Case A1 showing generator and battery power contribution

Fig. 5.8 shows the change in LMP of Bus 8 before and after performing DR. The LMP of bus 8 is reduced by a large amount during hours 9 ,10, 17, 18, 19 and 20 along with small reductions throughout the scheduling period. The case before DR where the lumped load and net data-center load are in the market inefficient zone, results in a system

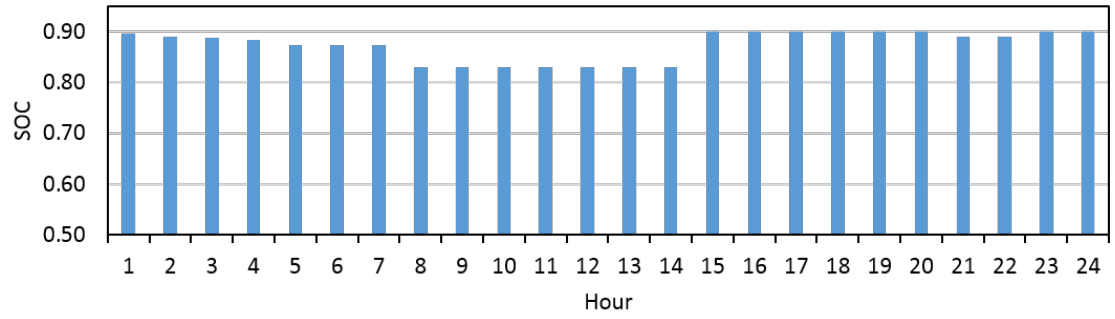

Figure 5.7. Case A1 showing variation of battery SOC

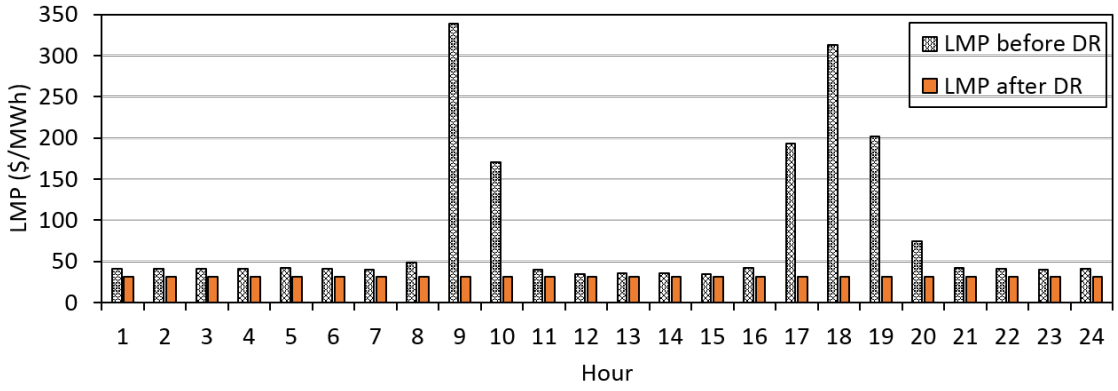

Figure 5.8. Case A1 showing change in LMP at Bus 8 as a result of DR

cost of $192,949. After performing DR, the system cost is $146,095, resulting in a total system saving of S_{sys} =$46,854, calculated from Eq. 4.3. VPP reduced the load of the data center by using the natural gas generators and batteries, optimally by solving Eq. 5.11. The total generator operation cost including fuel, startup and maintenance cost for the day-ahead DR response is $5,097, so the total energy savings as seen by the data center is S_{dc} =$37,663, calculated from Eq. 4.4.

5.3.2.2 Case A2: Using price curve P2

The simulation result using P2 as the price curve is shown by Fig. 5.9. The LMP price of the bus after DR reaches around 31.8 $/MWh, but this time the bus load is higher

(range 29 MW to 30 MW) in comparison to Case A1. It can be seen from Fig. 5.3, the LMP price of the node is less than 32 $/MWh up to bus load of 30 MW. So, there is no additional need for the data center energy resources to provide power during all time, except the peak hours as in case A1. However in this case, the battery throughout is 893 kWh, out of the total budgeted limit of 1780 kWh. This can be attributed to the constraint to maintain SOC at the end of the day to be 0.9, as the battery discharge requires corresponding charge to bring back the SOC to the original level. And in this case, the cost of charging the battery either through use of generator or grid will be increase the cost for data center.

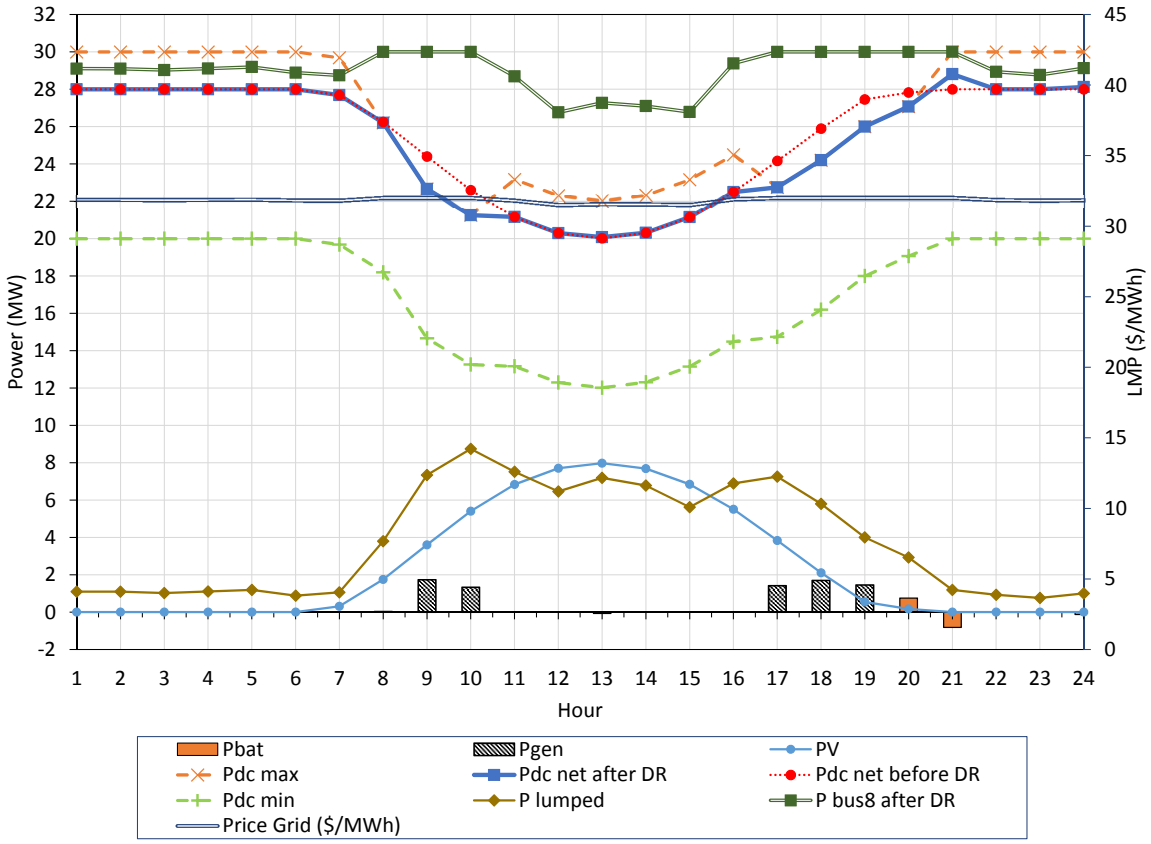

Figure 5.9. Case A2 overall scheduling result

5.3.2.3 Case A3: Using price curve P3

The simulation result using P3 as the price curve is shown by Fig. 5.10. In this case, the LMP of Bus 8 settles to around 32 $/MWh. But apart from Case A2, the LMP is higher after the bus power crosses 27 MW. This leads to more power from the generator as it is slightly cheaper than the grid. Also, the battery utilization is higher than from case A2, as 1709 kWh battery energy is used. It can be seen that battery is being discharged during peak hours 8 and 10, and is charged during non-peak hour at 11. In addition, the battery is charged by running the generator at maximum capacity at hour 17 to recover the SOC of battery.

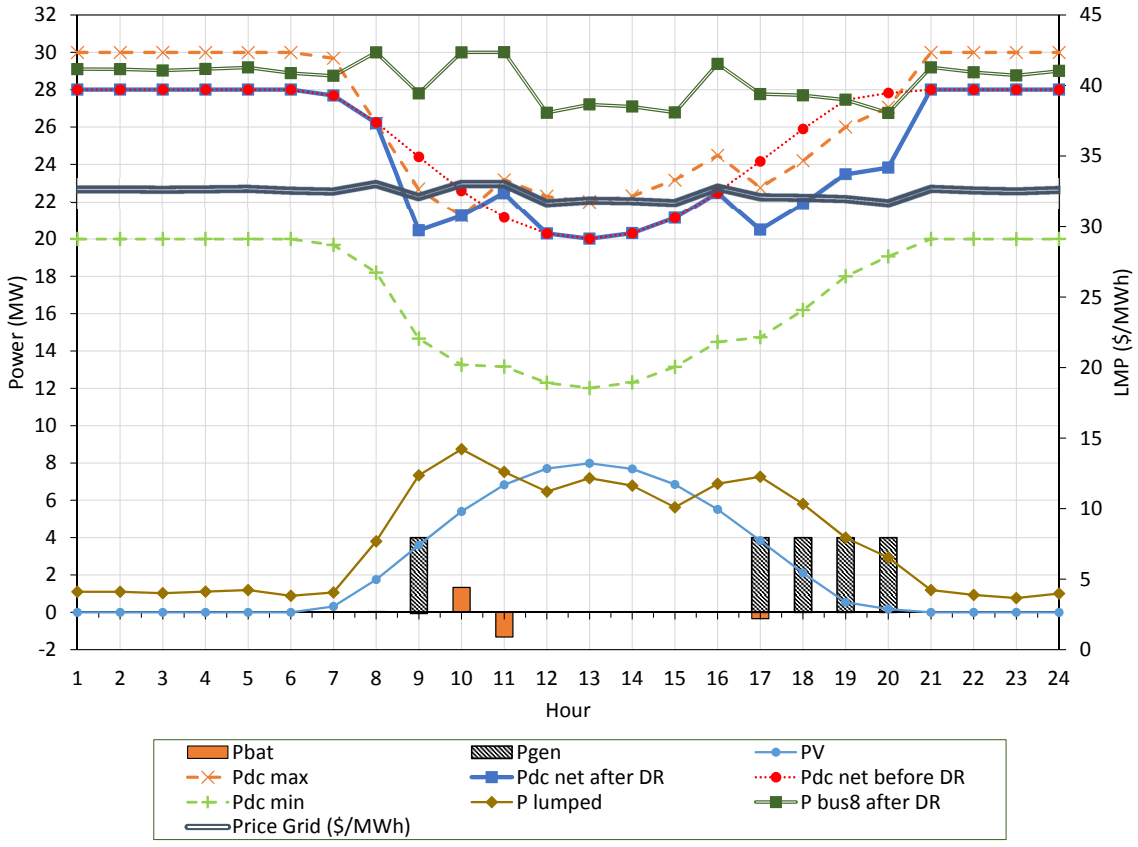

Figure 5.10. Case A3 overall scheduling result

5.3.3 Case B : 24 MW data center power

The data center in this case is assumed to be 24 MW. The lumped load has been scaled accordingly to induce peak load at certain hours at that bus, and also affecting the LMP of other buses as well. The difference from Case A1 is that during off-peak hours, like in the morning and the night, Bus 8 will have normal load so that the LMPs are normal during those times. In Case A1, maximum use of data center generators are required due to the high LMP in off-peak hours also. Fig. 5.11 shows the operating ranges provided by the ISO for the data center to operate denoted by P_{dcmax} and P_{dcmin}; net data center load before DR; solar power of data center; lumped load connected at the same bus; and total bus power. It shows that the market is inefficient during hours 9 and 10 in the morning and hours 17 through 19 in the evening. The ISO curtails the peak load through DR to make the market more efficient by removing congestion in the grid.

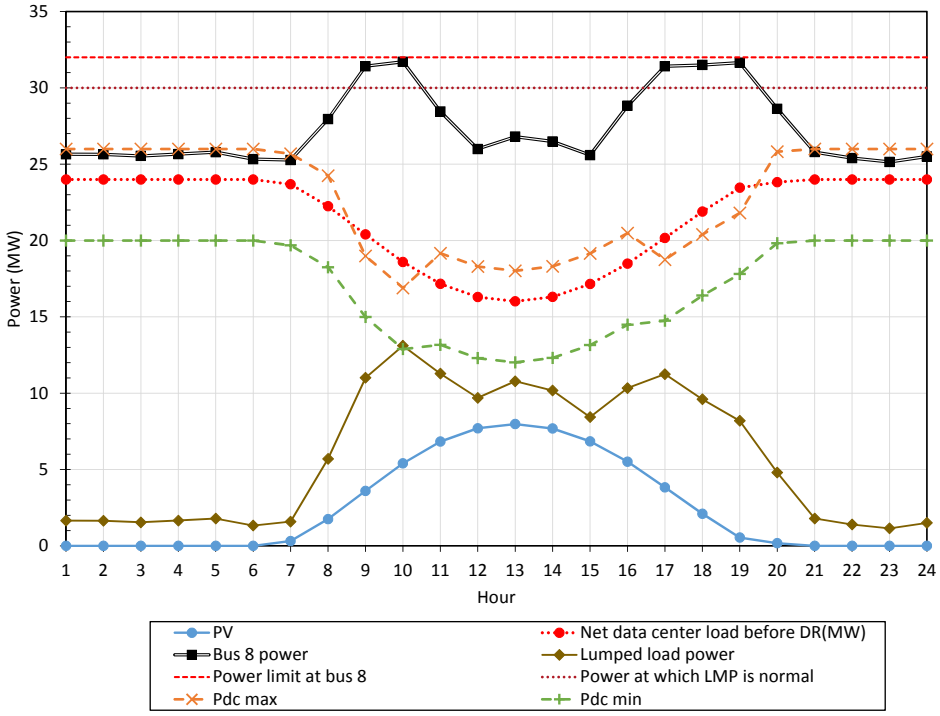

Figure 5.11. Case B input scenario

5.3.3.1 Case B1: Using price curve P1

The simulation result using P2 as the price curve is shown by Fig. 5.12. Comparing with case A1, it can be seen that during off-peak hours as in the morning and evening, the bus load is lower, so there is no necessity for data center's generator to be started, but in hours 2, 3, 6 and 7, some portion of battery energy has been scheduled by fully utilizing its allocated battery energy so as to bring down the LMP.

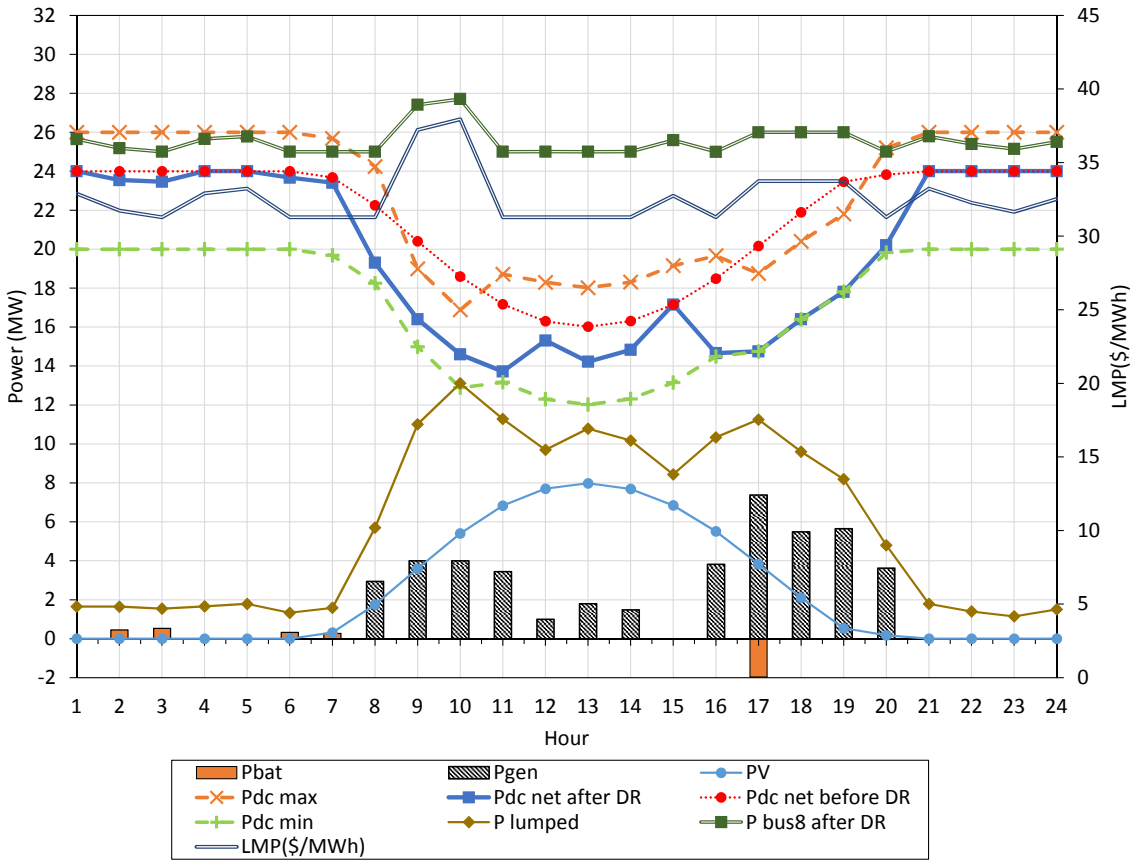

Figure 5.12. Case B1 output scenario

5.3.3.2 Case B2: Using price curve P3

The simulation result using P2 as the price curve is shown by Fig. 5.13. During hours 9, 10, 17, 18 and 19, the data center reduces the net load by using its generator and

battery energy power. The battery throughput is about 1743 kWh i.e, nearly all of the battery energy limit allocated for DR purpose is being used.

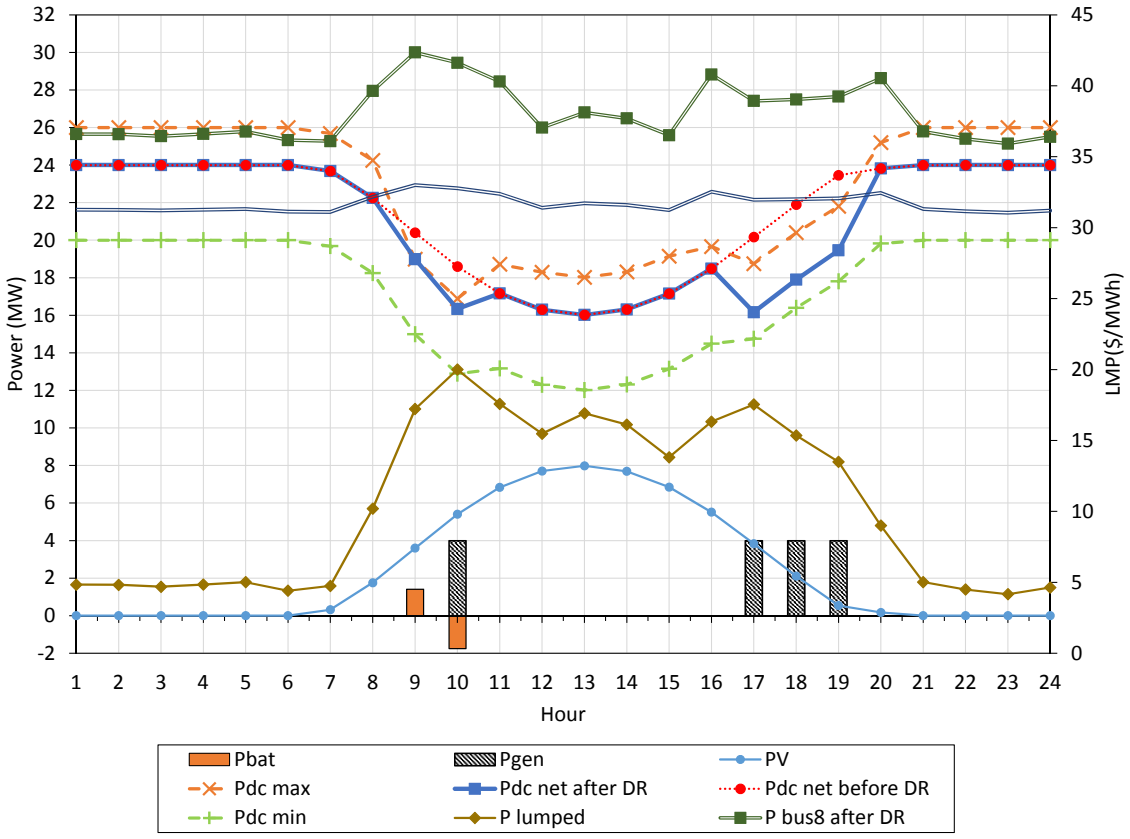

Figure 5.13. Case B2 output scenario

5.3.3.3 Case B3: Using price curve P3

In this case, to show that battery discharge above the budgeted limit can take place, a scenario is generated where the grid requires more power to be consumed by the load during night time. This can be due to increase of wind power during night time, and hence for maintaining frequency regulation, the data center may be asked for consuming more energy than its load by charging its battery bank. Fig. 5.14 shows a case where in hours 26, 27 and 28 require data center net power consumption to be at-least 25 MW. The

scheduling window has been changed from hour 5 to hour 28, i.e., hour 3 of next day.

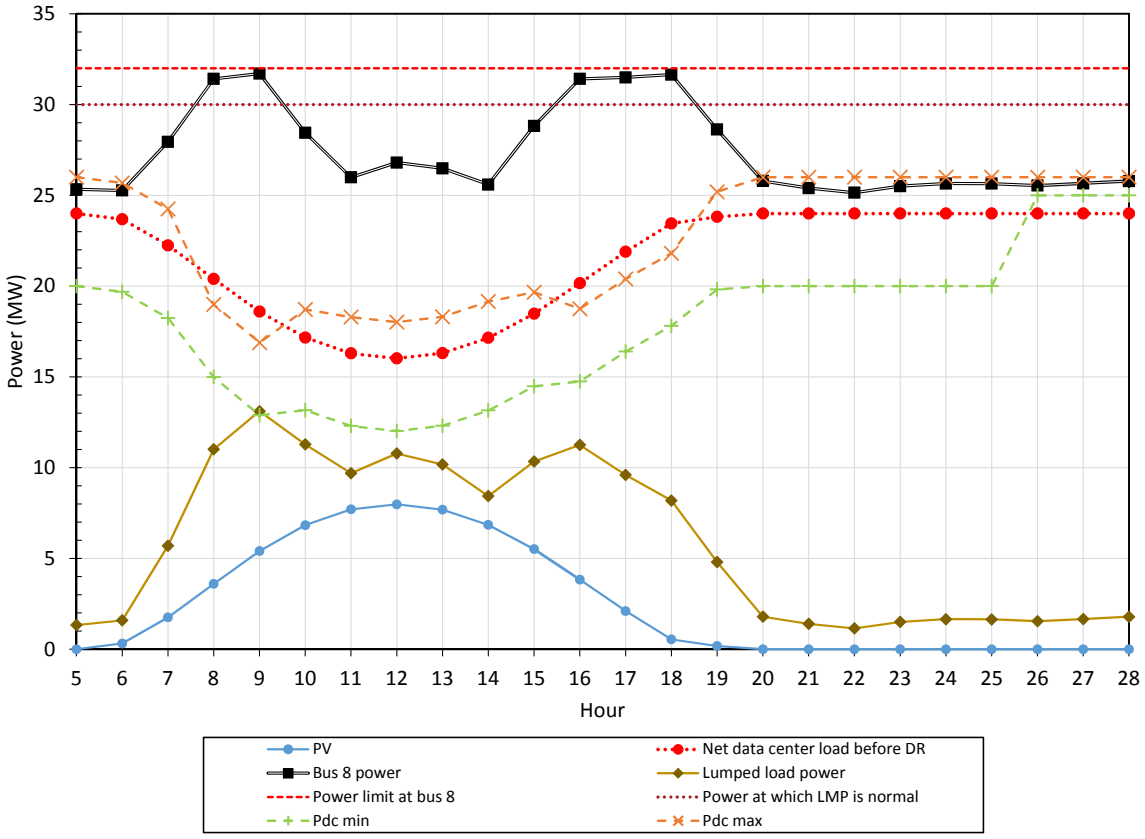

Figure 5.14. Case B3: data center required to consume power during night time

Fig. 5.15 shows the resulting scheduling output of generator and battery after solving the optimization model. The total throughput of the battery is 2700 kWh, which exceeded the battery budget limit of 1780 kWh by 920 kWh, resulting in battery wear cost of $365. The cost incurred by operation of battery above the budgeted limit can be recovered through the incentives provided by the ISO by taking part in power system support services. The battery bank reaches the lowest SOC of 0.78, indicating a DOD of 12.2% from the initial charge level as shown in Fig. 5.16

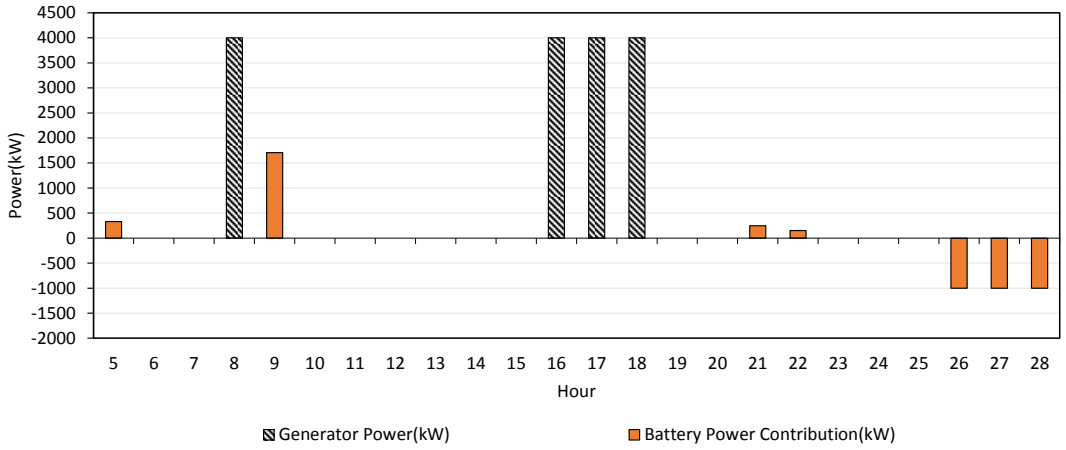

Figure 5.15. Scheduling of generators and battery

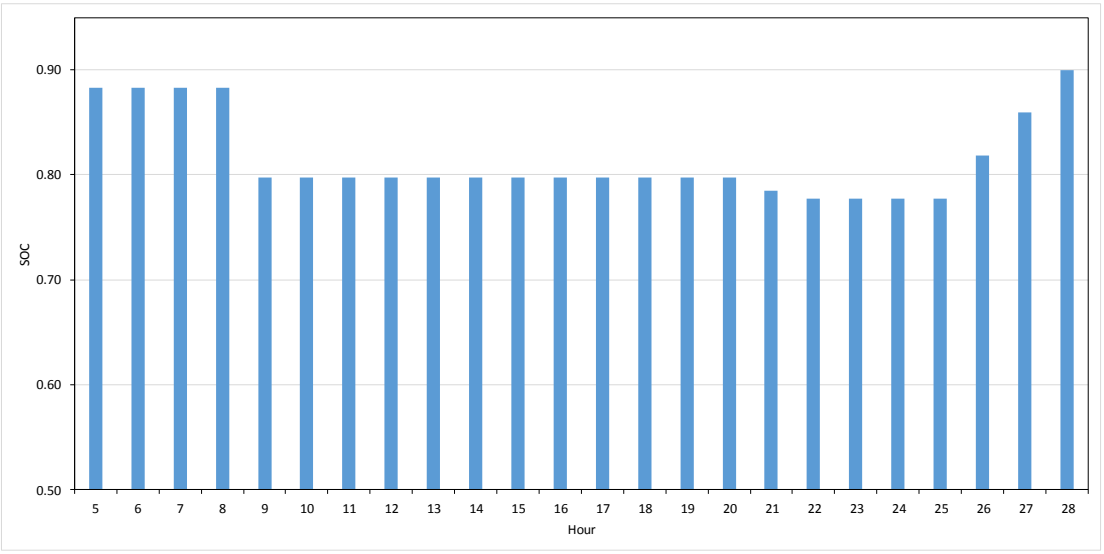

Figure 5.16. SOC variation of battery

5.4 Result and analysis

The results obtained from above cases show that data center's generator and battery energy can be utilized to reduce the peak load of the bus. It resulted in lower values of LMPs across all buses by removing the congestion in the grid, thereby improving market efficiency. In almost all the cases, the usage of battery is generally less than or equal to the

allocated battery energy limit. The reason for the battery usage to be less is because the battery needs to get recharged back to the starting charge level at the end of the scheduling window, and sometimes the cost of charging the battery increases the overall cost of operation of data center itself. It can be seen that the price of the grid and the price of data center's energy resources affect the scheduling decision to a greater extent. In Case A1, the data center's generators were scheduled whole day because it was cheaper to run its generator, instead of importing from the grid. However in Case A2 and A3, because of the use of the modified price curves, it was beneficial to import power from the grid, except the hours where LMP becomes very high. Case B is the same as Case A except the change in data center load and lumped load, which can happen in practical system. Case B1 and Case B2 were also analyzed using different price curves to see the effectiveness of the optimization model. In case B3, it was shown that if required, the battery can provide more energy than the budgeted limit by obeying all other constraints.

Therefore, based on the grid-operating range provided by the ISO, and the information regarding LMP, data center VPP can schedule its energy resources so as to assist the grid in reducing peak load as well as change the electricity consumption from the grid to lower the overall cost of data center operation.

CHAPTER 6 INTRODUCTION TO STOCHASTIC MODEL

In deterministic programming, all parameters are known with certainty. However, in real world, perfect information does not always exist. Stochastic programming is a useful method to deal with uncertainty of data either in the objective function or in constraints. In this chapter, a brief overview of stochastic optimization is described, and the methodology for scenario generation and reduction is explained along with a case study with the stochastic optimization model is presented for data center VPP. Further improvements in this chapter will be required in future works.

6.1 Stochastic optimization

PV variability is not included in the deterministic model. This may cause larger deviation during real-time scheduling. Since the exact forecast of PV cannot be available during the day-ahead period, decisions should be flexible enough to cope with the uncertainty. Uncertainties are represented through a number of reasonable realizations of an uncertain variable, which is solar power in this case. Scenarios can be used to incorporate uncertainties by including scenarios which have high probability of occurrence. Therefore in stochastic optimization, the expected value of the objective function is minimized over all the scenarios considered. A two-stage optimization framework is used to develop stochastic model. In the first stage, here–and–now or first stage variables – in this case, ON/OFF status of generators, that is common to all scenarios is determined. In the second stage, wait–and–see or second stage variables – in this case, generator power and battery power, takes different values based on each scenarios. The scenarios are critical inputs as it will negatively affect the outcome of

stochastic optimization if reasonable scenarios are not considered.

6.1.1 Scenario generation

Stochastic variables cannot be represented by a continuous function as the number of scenarios will be infinite. There are scenario generation algorithms that will develop a large number of discrete realizations of a stochastic variable. The forecasting error probability distribution function can be used to develop a number of scenarios using Monte Carlo method. The PV error scenarios are generated assuming normal distribution. Based on the range of prediction interval (PI) which is typically 95% of the probabilistic confidence interval, scenarios can be generated. The minimum and maximum range of PV fluctuation can be determined as shown in Eq. 6.1 if the forecasting error distribution is assumed to be normally distributed with mean, μ_{error}, and standard deviation, σ_{error}, with z-score value of 1.96 for a confidence interval of 95%.

$$range = \pm(\mu_{error} + z \times \sigma_{error}) \tag{6.1}$$

6.1.2 Scenario reduction

Scenario generation usually produces a large number of scenarios. This increases the problem size considerably and may result in intractability of the developed stochastic model. Even if it is solvable, the computational burden will be too high for it to solve with a reasonable amount of time. Therefore, scenario reduction technique is employed to reduce the size of the scenarios. There is a trade–off between use of high number of scenarios and lower number of scenarios. High number of scenarios will typically capture all the variations of the stochastic inputs but will increase computation time, whereas

fewer scenarios quickly yield a solution, but may risk losing information. So, generally in scenario reduction algorithm, low probability scenarios are eliminated, and similar scenarios are merged to become one by transferring of their probabilities value to the merged scenario. In this thesis, fast-forward method of scenario reduction, known as Kantorovich distance [46], is used to reduce the scenario generated through Monte Carlo method.

6.2 Stochastic optimization model

Two stage decision framework is implemented for stochastic optimization [47]. In the first stage, generator ON/OFF decision is made before the realization of PV uncertainty. In the next stage, based on the first stage decisions and the realization of different scenarios, power output from the generator and battery is determined. It minimizes the expected objective function considering all the available scenarios. The stochastic objective function for data center VPP optimization is given by Eq. 6.2.

$$\begin{aligned}\min_{P_{Gi,S},U_i,P_{Bat,S}} \sum_{s=1}^{S} \Pi_S \{ (\sum_{t=1}^{T} (\sum_{i=1}^{N_g} C_i(P_{Gi,t}^S) + MC \times U_{i,t} + SUP \times Y_{i,t}) \\ + LMP_{grid,t}^S \times P_{dcNetLoad,t}^S) + C_{batWear} \times P_{batExtra}^S \}\end{aligned} \tag{6.2}$$

where, Π_S is the probability of each scenarios S, $P_{Gi,t}^S$ is the power output of generator i at time t for each scenario, $P_{batExtra}^S$ is the extra battery energy output for each scenario, $P_{dcNetLoad,t}^S$ is the net data center load at time t for each scenario. All other constraints are the same as in Eq. 5.12 through Eq. 5.19, with the inclusion of scenarios in each of them.

6.3 Test case

The input for this test case is Case A1 presented in Section 5.3.2.1, but in this case, ten scenarios of PV power are used instead of one the deterministic case.

6.3.1 Scenario for PV power

The solar power forecast is performed using Markov Switching Model (MSM) developed in [48]. At first, using the irradiance data for Colorado, power from the solar panel were calculated using Eq. 3.1. The mean and standard deviation of solar forecast error for the whole month of July was determined. The maximum and minimum range, or the prediction interval is evaluated based on the z-value, forecasted value, mean error and standard deviation as given by Eq. 6.1. Fig. 6.1 shows the error distribution of the solar forecast error for the month of July, 2005.

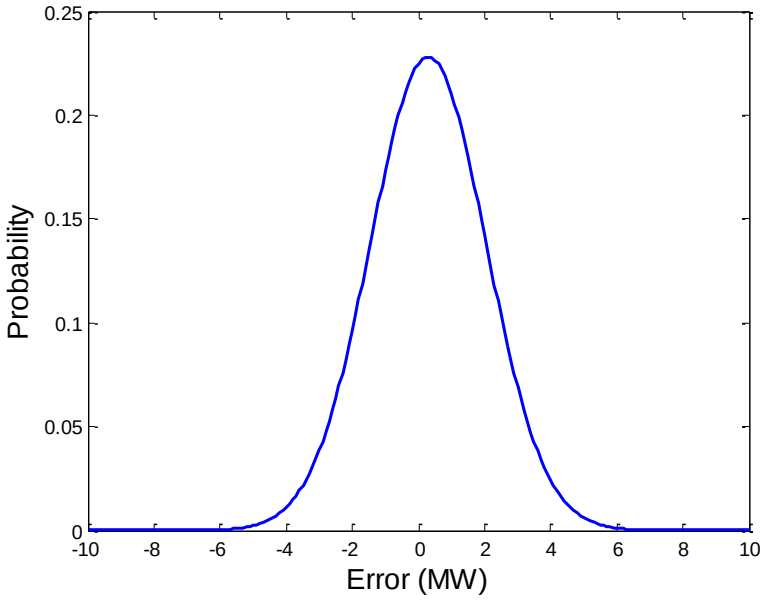

Figure 6.1. Normal distribution of solar forecast error for the month of July, 2005

After determining the range of solar power output, Monte Carlo simulation method was performed to generate random 1,000 scenarios for a day with each scenario having equal probability of 0.001, as shown in Fig. 6.2. Kantorovich distance scenario reduction method was then applied to reduce 1,000 scenarios to just ten , with each reduced scenario having adjusted probabilities, which is shown in Fig. 6.3.

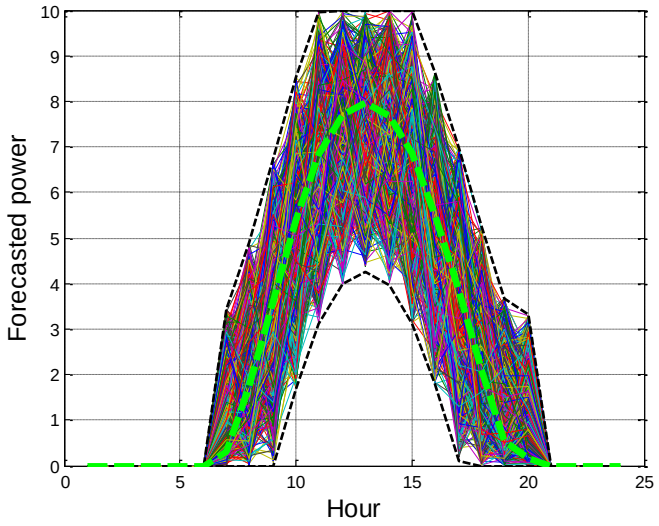

Figure 6.2. Scenario generation using Monte Carlo Simulation method

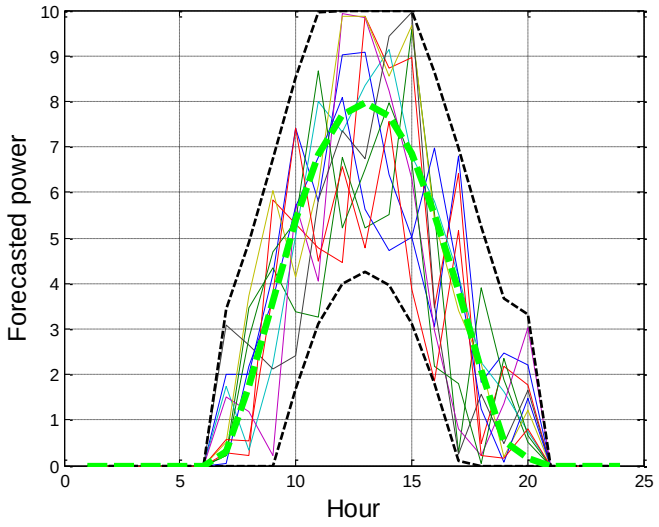

Figure 6.3. Scenario reduction using Kantorovich distance method

6.4 Result and analysis

IBM ILOG CPLEX mixed integer programming (MIP) was used to solve the stochastic optimization for ten different scenarios for PV output. The simulation time took about 3.6 hours to solve using INTEL Core 2 Quad CPU running at 2.83 GHz with MIP tolerance of 2%. The expected value of the objective function, which is the expected minimum data center operational cost was found to be $23,319. Fig. 6.4 shows the generator and battery scheduling for the highest probability scenario along with the loadings at Bus 8.

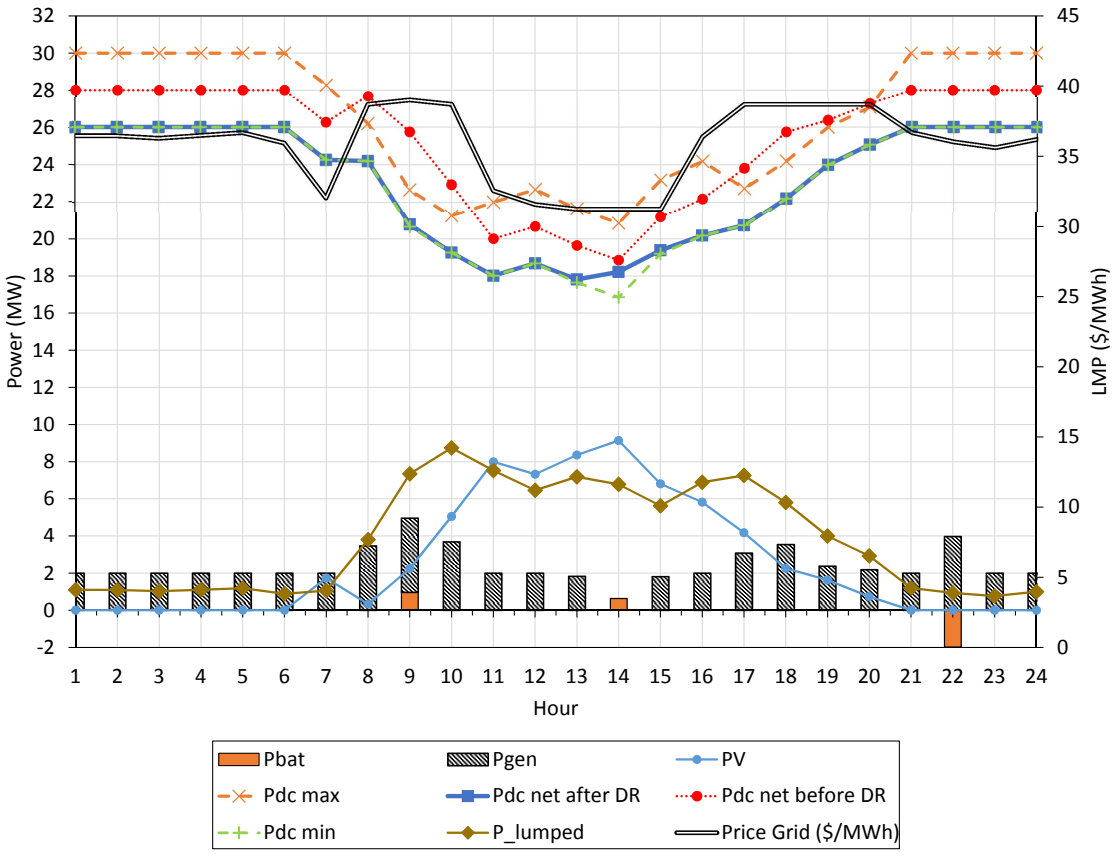

Figure 6.4. Generator and battery scheduling for a particular scenario

In previous chapters, deterministic scheduling was performed in which it considered

PV power to be known with full certainty. Stochastic optimization is required to account for the uncertainty in the variables by using a number of scenarios, which yields a solution that is in average suitable for all the input scenarios. To study the effectiveness of the stochastic optimization, a real-time dispatch needs to be performed to see if there is difference in the day-ahead scheduling decisions and real-time decisions. The cost associated with real-time dispatch may vary with the average cost if the scenarios considered deviate greatly during real-time. In this thesis, real-time dispatch layer has not been implemented, and can be added in the future to study the effectiveness of the day-ahead stochastic model, and also implement the data center VPP EMS model in real-time.

CHAPTER 7 CONCLUSIONS

7.1 Summary

Data centers represent a large load for the grid, and there are a large number of data centers scattered spatially across the grid. The cost associated with the electricity consumption of the data center is large. In addition, transmission network in the grid is becoming congested as a result of load growth. Also, the LMP across the buses are abnormally high during peak load periods as a result of transmission congestion, which requires operation of expensive peaking generating power plants.

In this thesis, the underutilized data center energy resources such as backup generator and UPS battery storage, along with the renewable energy source are combined to form a VPP, and the EMS controls scheduling decision of all the DERs of the data center. The data center's EMS can communicate with the ISO about the grid conditions in the day-ahead market, and can know the range of operation of the data center to schedule the generators and battery power based on data center load, renewable generation output and the impact of its net load on the LMP price of the bus connected to the data center. Different set of LMP price curves are used to study its effect on the scheduling decision of the generator and battery. It can be concluded that data center tries to use its generators unless importing from the grid is the cheap option. Also, the data center tries to consume nearly all of its allocated battery energy if it can be recharged back to its original SOC at the end of the scheduling period without costing more for the data center. The way in which DOD for DR purpose was determined so that it would not affect the float life of the battery, led to a more safer condition for battery in terms of the battery charge available

for the power outage. In no case was the SOC of the battery was lower than 0.81, which ensured the battery can supply during power outage scenario until the back up generators come into operation and handle the full load of the data center.

Economic saving calculation was performed in the modified IEEE-30 bus test system. It was found that performing DR during peak load periods resulted in economic savings to the system as well as to the data center itself. Also, reducing the data center load at other off-peak hours also resulted in savings to the data center itself in the form of reduced electricity bill.

7.2 Conclusions

A data center is a large, flexible load that can operate as a VPP and participate in DR programs, benefiting both the system and the data center. For the system, the VPP DR cuts off the peak load which can reduce congestion in the transmission network and also avoid expensive peaking generators from operating. Additionally, the VPP DR results in a lower electricity cost for the wholesale market. For the data center, the owner can avoid paying a much higher electricity rate during high LMP period and thus provide energy cost savings. Battery energy can be utilized to supply a predefined allocated energy during DR period without causing additional cost and degradation of the battery. The savings by the data center participating in the DR program far outweighs the expense due to operating its own generators and battery.

7.3 Future work

The stochastic optimization may consider variation of data center load, in addition to the variation of PV power. Also, real-time scheduling system should be developed to

study the effectiveness of the proposed day-ahead stochastic model. Further, a suitable model for providing data center the reward for performing the DR by the ISO can be considered. It would be interesting to see a multi-VPP coordination between data centers located at different locations, and include workload shifting in addition to utilizing backup energy resources for changing the data center load profile.

REFERENCES

[1] B Baker, *Microsoft, Apple, Google power data centers with renewable energy*, Accessed: Oct. 19, 2015. [Online]. Available: http://ecowatch.com/2013/11/04/tech-companies-renewables-combat-data-center-energy-crisis/.

[2] National Resources Defense Council, "Data center efficiency assessment," Aug. 2014.

[3] United States Energy Information Administration, "Annual energy outlook 2015," Apr. 2015.

[4] J. Osborne and D. Warrier, "A primer on demand response - the power grid: Evolving from a dumb network to a smart grid," *Thomas Weisel Partners Equity Research*, 2007.

[5] Federal Energy Regulatory Commission, "A assessment of demand response potential," *Prepared by The Brattle Group, Freeman Sullivan, & Co, and Global Energy Partners*, 2009.

[6] W. P. Turner IV, J. PE, P. Seader, and K. Brill, "Tier classification define site infrastructure performance," *Uptime Institute*, vol. 17, 2006.

[7] P. Lombardi, M. Powalko, and K. Rudion, "Optimal operation of a virtual power plant," in *IEEE Power Energy Society General Meeting*, 6 pp, 2009.

[8] J. Li, Z. Bao, and Z. Li, "Modeling demand response capability by internet data centers processing batch computing jobs," *IEEE Transactions on Smart Grid*, vol. 6, no. 2, pp. 737–747, 2015.

[9] M. Polverini, A. Cianfrani, S. Ren, and A. V. Vasilakos, "Thermal-aware scheduling of batch jobs in geographically distributed data centers," *IEEE Transactions on Cloud Computing*, vol. 2, no. 1, pp. 71–84, 2014.

[10] Y. Yao, L. Huang, A. B. Sharma, L. Golubchik, and M. J. Neely, "Power cost reduction in distributed data centers: A two-time-scale approach for delay tolerant workloads," *IEEE Transactions on Parallel and Distributed Systems*, vol. 25, no. 1, pp. 200–211, 2014.

[11] R. Wang, N. Kandasamy, C. Nwankpa, and D. R. Kaeli, "Datacenters as controllable load resources in the electricity market," in *2013 IEEE 33rd International Conference on Distributed Computing Systems (ICDCS)*, 2013, pp. 176–185.

[12] A. Wierman, Z. Liu, I. Liu, and H. Mohsenian-Rad, "Opportunities and challenges for data center demand response," in *2014 International Green Computing Conference (IGCC)*, 10 pp, 2014.

[13] R. Urgaonkar, B. Urgaonkar, M. J. Neely, and A. Sivasubramaniam, "Optimal power cost management using stored energy in data centers," in *Proceedings of the ACM SIGMETRICS Joint International Conference on Measurement and Modeling of Computer Systems*, ACM, pp. 221–232, 2011.

[14] Z. Liu, A. Wierman, Y. Chen, B. Razon, and N. Chen, "Data center demand response: Avoiding the coincident peak via workload shifting and local generation," *Performance Evaluation*, vol. 70, no. 10, pp. 770–791, 2013.

[15] C. Pfeiffer, P. Maltbaek, and E. Kulali, *System and method for using data centers as virtual power plants*, US Patent App. 13/565,724, 2012.

[16] E. Mashhour and S. M. Moghaddas-Tafreshi, "Bidding strategy of virtual power plant for participating in energy and spinning reserve markets - Part I: Problem formulation," *IEEE Transactions on Power Systems*, vol. 26, no. 2, pp. 949–956, 2011.

[17] S Awasthi, S Chalise, and R Tonkoski, "Operation of data center as a virtual power plant," in *2015 IEEE Energy Conversion Congress and Exposition (ECCE)*, 6 pp, Sep. 2015.

[18] D. Wang, C. Ren, A. Sivasubramaniam, B. Urgaonkar, and H. Fathy, "Energy storage in datacenters: What, where, and how much?" In *ACM SIGMETRICS Performance Evaluation Review*, vol. 40, 2012, pp. 187–198.

[19] V. Kontorinis, L. E. Zhang, B. Aksanli, J. Sampson, H. Homayoun, E. Pettis, D. M. Tullsen, and T. S. Rosing, "Managing distributed ups energy for effective power capping in data centers," in *2012 39th Annual International Symposium on Computer Architecture (ISCA)*, pp. 488–499, 2012.

[20] B. Aksanli, T. Rosing, and E. Pettis, "Distributed battery control for peak power shaving in datacenters," in *2013 International Green Computing Conference (IGCC)*, IEEE, 8 pp, 2013.

[21] L. Narayanan, D. Wang, A.-A. Mamun, A. Sivasubramaniam, and H. K. Fathy, "Should we dual-purpose energy storage in datacenters for power backup and demand response?" In *6th Workshop on Power-Aware Computing and Systems (HotPower 14)*, 2014.

[22] A Dauensteiner, "European virtual fuel cell power plant," *Management Summary Report*, 2007.

[23] D. Pudjianto, C. Ramsay, and G. Strbac, "Virtual power plant and system integration of distributed energy resources," *Renewable power generation, IET*, vol. 1, no. 1, pp. 10–16, 2007.

[24] N. Research, *Virtual power plants demand response, supply-side, and mixed asset VPPs: Global market analysis and forecasts*, Accessed: Jan 5, 2016. [Online]. Available: https://www.navigantresearch.com/research/virtual-power-plants.

[25] C. Ramsay, "The virtual power plant: Enabling integration of distributed generation and demand," *FENIX Bulletin 2*, 2008.

[26] H Saboori, M Mohammadi, and R Taghe, "Virtual power plant (vpp), definition, concept, components and types," in *2011 Asia-Pacific Power and Energy Engineering Conference (APPEEC)*, 4 pp, 2011.

[27] G. Cook and J. Van Horn, "How dirty is your data? a look at the energy choices that power cloud computing," *Greenpeace (April 2011)*, 2011.

[28] G. Ghatikar, "Demand response opportunities and enabling technologies for data centers: Findings from field studies," LBNL, 2014.

[29] PVeducation.org, *Short-circuit current —PVeducation*, Accessed: Jan 21, 2016. [Online]. Available: http://www.pveducation.org/pvcdrom/solar-cell-operation/short-circuit-current.

[30] S. McCluer and J.-F. Christin, "Comparing data center batteries, flywheels, and ultracapacitors," *White paper*, vol. 65, 2008.

[31] R. Zimmerman, C. Murillo-Sánchez, and R. Thomas, "Matpower: Steady-state operations, planning, and analysis tools for power systems research and education," *IEEE Transactions on Power Systems*, vol. 26, no. 1, pp. 12–19, 2011.

[32] Lawrence Berkeley National Laboratory, "Benchmarking: Data centers - Case Study Reports," [Online]. Available: http://hightech.lbl.gov/.

[33] *National Solar Radiation Database (NSRDB)*, 2015. [Online]. Available: https://nsrdb.nrel.gov/nsrdb-viewer.

[34] D. Erbs, S. Klein, and J. Duffie, "Estimation of the diffuse radiation fraction for hourly, daily and monthly-average global radiation," *Solar Energy*, vol. 28, no. 4, pp. 293–302, 1982.

[35] J. A. Duffie and W. A. Beckman, *Solar engineering of thermal processes*. Wiley New York etc., 1980, vol. 3.

[36] "Costs of Utility Distributed Generators, 1-10 MW: Twenty-Four Case Studies," EPRI, Palo Alto, CA and Cooperative Research Network, Arlington, VA, Tech. Rep., 2003.

[37] *CAT gas generator set*, Accessed: Nov 21, 2015. [Online]. Available: http://www.cat.com.

[38] National Renewable Energy Laboratory, *NREL RSF measured data 2011*, Accessed: Jan 5, 2016. [Online]. Available: http://en.openei.org/datasets/dataset/nrel-rsf-measured-data-2011.

[39] R. Ferrero, S. Shahidehpour, and V. Ramesh, "Transaction analysis in deregulated power systems using game theory," *IEEE Transactions on Power Systems*, vol. 12, no. 3, pp. 1340–1347, 1997.

[40] O. Alsac and B. Stott, "Optimal load flow with steady-state security," *IEEE Transactions on Power Apparatus and Systems*, vol. PAS-93, no. 3, pp. 745–751, 1974.

[41] *Electric Power Annual*, Accessed: Oct 15, 2015. [Online]. Available: http://www.eia.gov/electricity/annual/html/.

[42] HOMER Energy, *Homer pro 3.3*, Accessed: Nov. 4, 2015. [Online]. Available: http://www.homerenergy.com.

[43] M. Dubarry, V. Svoboda, R. Hwu, and B. Y. Liaw, "Capacity and power fading mechanism identification from a commercial cell evaluation," *Journal of Power Sources*, vol. 165, no. 2, 566–572, 2007.

[44] S. Drouilhet and B. L. Johnson, "A battery life prediction method for hybrid power applications," in *AIAA Aerospace Sciences Meeting and Exhibit*, 1997.

[45] K. H. LaCommare, "Tracking the reliability of the us electric power system: An assessment of publicly available information reported to state public utility commissions," *Lawrence Berkeley National Laboratory*, 2008.

[46] H. Heitsch and W. Römisch, "Scenario reduction algorithms in stochastic programming," *Computational optimization and applications*, vol. 24, no. 2-3, pp. 187–206, 2003.

[47] P. A. Ruiz, C. R. Philbrick, E. Zak, K. W. Cheung, and P. W. Sauer, "Uncertainty management in the unit commitment problem," *IEEE Transactions on Power Systems*, vol. 24, no. 2, pp. 642–651, 2009.

[48] A. Shakya, S. Michael, C. Saunders, D. Armstrong, P. Pandey, S. Chalise, and R. Tonkoski, "Solar irradiance forecasting in remote microgrids using Markov switching model," *IEEE Transactions on Sustainable Energy*, 2016, to be published.